

Prediction of protein assemblies, the next frontier: The CASP14-CAPRI experiment

**Marc F. Lensink,
Guillaume Brysbaert, Nurul Nadzirin, Sameer Velankar,
all CAPRI participants and Shoshana J. Wodak**

Supplementary Material

– Funding	2
– Table S1 – Participation statistics	3
– Table S2 – Prediction results	4
<p>The Table lists for every interface the performance of CAPRI and CASP Predictor groups, Server groups and Scorer groups. Scorer groups include human predictor groups and automated servers, with the latter listed in all capitals. Results are listed as the number of submitted models of acceptable quality or better, with the number of higher than acceptable quality models listed after a slash, <i>e.g.</i> '5/4**' indicates that 9 models of acceptable quality or better were submitted, of which 4 are of medium quality. Only the first five models of a submission were considered. Incorrect models are not listed.</p>	
– Table S3 – Prediction performance for assembly targets	24
<p>The Table lists for every assembly target the quality of the best model for each of the 9 (T170), 3 (T177) or 2 (T180) interfaces. Results are listed for the groups as in Table S2 and the last column sums over the various interfaces, <i>e.g.</i> '6/2**' indicates that for 6 interfaces a model of acceptable quality or better was produced and for two of these the model was of medium quality. Only the first five models of a submission were considered.</p>	
– Table S4 – Participant performance	27
– Table S5 – Interface prediction accuracy	28
– Individual Group Summaries – Methods employed by the CAPRI participants	29
<p>I Bates – Protein complex assembly by employing particle swarm optimization</p> <p>II Chang – Summary, Chang group, CAPRI Round 50 (CASP14-CAPRI)</p> <p>III Cheng – Reconstructing protein complex structure from predicted inter-chain contacts in CAPRI-Round 50</p> <p>IV Czaplewski – Extended abstract: UNRES group¹</p> <p>V Del Carpio – Incorporating flexibility by soft docking in MIAX</p> <p>VI Gray – Rosetta docking strategies in the CASP14-CAPRI experiment</p> <p>VII HADDOCK – HADDOCK scoring of CAPRI Round50 models</p> <p>VIII CLUSPRO – Hybrid ClusPro approach in 2020 CASP-CAPRI round: template-assisted docking and docking of protein models</p> <p>IX Fernandez-Recio – Fernandez-Recio's group performance in CASP14 / CAPRI round 50</p> <p>X Grudinin – Quaternary structure prediction using a combination of physics-based approaches with machine learning</p> <p>XI Huang – Integrating residue-residue contact prediction and hybrid scoring function into hybrid docking in CASP14-CAPRI</p> <p>XII Kihara / LZERD – Kihara human team and LZerD server performance in CAPRI 50 / CASP 14</p> <p>XIII Nakamura – Template-based structure prediction and inter-residue distances and orientations prediction-based structure prediction</p> <p>XIV Pierce – CAPRI Round 50 extended abstract, Pierce team</p> <p>XV Oliva – Oliva Team performance, CASP14-CAPRI, Round 50</p> <p>XVI Shen – Performance of the Shen team in CASP14-CAPRI Round 50</p> <p>XVII Seok – Predicting protein complex structures using GALAXY in CAPRI round 50</p> <p>XVIII Takeda-Shitaka – Performance of Takeda-Shitaka team in CASP14-CAPRI Round 50</p> <p>XIX Vakser – Modeling CAPRI and oligomeric CASP targets by template-based and free docking</p> <p>XX Venclovas – Modeling of protein complexes in CAPRI Round 50</p> <p>XXI Zou / MDOCKPP – Summary of the Zou group and the MDOCKPP server</p>	

¹CAPRI group "Czaplewski" corresponds to UNRES.template in the abstract text

Funding information

- I. Bates - This research was funded in whole, or in part, by the Wellcome Trust (FC001003). For the purpose of Open Access, the author has applied a CC BY public copyright licence to any Author Accepted Manuscript version arising from this submission. RAGC, TC and PAB are funded and supported by the Francis Crick Institute, which receives its core funding from Cancer Research UK (FC001003), the UK Medical Research Council (FC001003), and the Wellcome Trust (FC001003).
- II. Chang - National Natural Science Foundation of China (81603152); Changzhou Science and Technology Bureau (CE20200503).
- III. Cheng – This work is supported in part by Department of Energy grants (DE-AR001213, DE-SC0021303, DE-SC0020400), NSF grants (DBI 1759934, IIS1763246), NIH grant (R01GM093123), and the computing allocation on the Summit supercomputer provided by Oak Ridge Leadership Computing Facility (Project ID BIF132).
- IV. Supported by National Science Center of Poland (Narodowe Centrum Nauki) (NCN), grants UMO-2017/25/B/ST4/01026, UMO-2017/26/M/ST4/00044, and UMO-2017/27/B/ST4/00926. Computational resources were provided by (a) the Interdisciplinary Centre of Mathematical and Computational Modelling (ICM) at the University of Warsaw (b) the Centre of Informatics Tricity Academic Supercomputer & Network (CI TASK) in Gdansk, (c) the Polish Grid Infrastructure (PL-GRID), and (d) our Beowulf cluster at the Faculty of Chemistry, University of Gdansk.
- V. –
- VI. US National Institutes of Health grant R01-GM078221.
- VII. The HADDOCK team acknowledges financial support from the European H2020 e-Infrastructure grants BioExcel (Grant No. 675728 and 823830), EOSC-hub (Grant No. 777536) and from the Dutch Foundation for Scientific Research (NOW) (TOP-PUNT Grant 718.015.001).
- VIII. This work was supported by grants DBI 1759277 and AF 1645512 from the National Science Foundation, and R35GM118078, R21GM127952, and RM1135136 from the National Institute of General Medical Sciences.
- IX. Grant PID2019-110167RB-I00 (Spanish Ministry of Science and Innovation).
- X. AK was supported by an Inria Cordi-S grant.
- XI. –
- XII. National Institutes of Health (R01GM133840, R01GM123055) and the National Science Foundation (CMMI1825941, MCB1925643, DBI20036350). CC was supported by a NIGMS-funded predoctoral fellowship (T32GM132024).
- XIII. This work was supported by the Japan Society for the Promotion of Science KAKENHI (Grant Number JP19J00950 to TN). Computations were partially performed on the ToMMo supercomputer system in Tohoku University, the Reedbush System in the Information Technology Center, the University of Tokyo, and the NIG supercomputer at ROIS National Institute of Genetics.
- XIV. –
- XV. –
- XVI. The study was in part supported by the United States National Institutes of Health (R35GM124952 to YS) and National Science Foundation (CCF-1943008 to YS).
- XVII. –
- XVIII. –
- XIX. NIH grant R01GM074255 and NSF grant DBI1917263.
- XX. Research Council of Lithuania (grants S-MIP-17-60 and S-MIP-21-35).
- XXI. NIH grants R01GM109980 (XZ), NIH R35GM136409 (XZ) and NIH R01HL142301 (to Jonathan R Silva).

Table S1 – Participation statistics

CAPRI ID	CASP ID	Stoichiometry	#interfaces	Predictors	Uploaders	Scorers	CASP
T164	T1032	A2	1	28	18	23	21
T165	H1036	A:HL	1	27	12	22	25
T166	H1045	AB	1	24	16	19	26
T168	T1052	A3	1	24	11	20	20
T169	T1054	A2	1	27	16	20	22
T170	H1060	A6B12C3D6	9	23	12	17	16
T174	T1070	A3	1	24	13	19	21
T176	T1078	A2	1	27	16	21	23
T177	H1081	A20	3	24	12	18	23
T178	T1083	A2	1	26	13	19	23
T179	T1087	A2	1	25	13	19	22
T180	T1099	A4	2	25	11	18	20

Target and participation statistics. Stoichiometry and #interfaces refer to the assessment entity. Predictors indicates the number of predictor groups uploading submissions. Whereas all predictor models enter the Scoring experiment, the number of Uploader groups indicates the number of predictor groups that submitted more than 10 models. The number of CASP groups excludes the CAPRI groups that also registered with CASP.

Table S2 – Prediction results for Target/Interface T164.1

Predictors	Top-1	Top-5
Gray	1	5/1**
Seok	1	4/1**
Zou	1	5
Venclovas	1	5
Kihara	1	5
Chang	1	5
Bates	1	5
Shen	1	4
Pierce	1	4
Kozakov/Vajda	0	4
Huang	1	4
Nakamura	1	3

CASP-only Predictors	Top-1	Top-5
<i>CoDock</i>	1	5
<i>htjcadd</i>	1	4
<i>Baker</i>	1	4
<i>Takeda-Shitaka</i>	0	2
<i>DATE</i>	1	2
<i>Risoluto</i>	1	1
<i>Elofsson</i>	1	1

Servers	Top-1	Top-5
MDOCKPP	1	4/1**
SWARMDOCK	1	5
HDOCK	1	4
HAWKDOCK	1	4
CLUSPRO	0	4
GALAXYPPDOCK	1	3
LZERD	0	2

Scorers and Scoring Servers	Top-1	Top-5
MDOCKPP	1	5/1**
SWARMDOCK	1**	5/1**
Huang	1**	5/1**
Bates	1**	5/1**
HDOCK	1	4/1**
Zou	1	5
Kihara	1	5
LZERD	1	5
Takeda-Shitaka	1	5
Bonvin	1	5
Shen	1	5
HAWKDOCK	1	5
Chang	1	4
Oliva	1	4
Grudin	0	3
Fernandez-Recio	0	2
PYDOCKWEB	0	2

Table S2 – Prediction results for Target/Interface T165.1

Predictors	Top-1	Top-5
<i>no acceptable models</i>		
CASP-only Predictors	Top-1	Top-5
<i>no acceptable models</i>		
Servers	Top-1	Top-5
<i>no acceptable models</i>		
Scorers and Scoring Servers	Top-1	Top-5
<i>no acceptable models</i>		

Table S2 – Prediction results for Target/Interface T166.1

Predictors	Top-1	Top-5
Vakser	1**	5**
Kozakov/Vajda	1**	5**
Huang	1**	5**
Chang	1	5/3**
Venclovas	0	1***
Shen	1**	3**
Fernandez-Recio	1**	3**
Bates	1**	3**
Zou	1**	5/1**
Pierce	1**	3/2**
Kihara	1**	5/1**
Seok	1	2/1**
Nakamura	0	1**
CASP-only Predictors	Top-1	Top-5
<i>Takeda-Shitaka</i>	1**	5/1***/4**
<i>Baker</i>	1**	5/1***/4**
<i>A/LON</i>	1**	5/4**
<i>CoDock</i>	1	5/3**
<i>DellaCorte</i>	1	4
<i>Lamoureux</i>	1**	1**
<i>DATE</i>	0	1**
Servers	Top-1	Top-5
MDOCKPP	1	5
SWARMDOCK	0	2
GALAXYPPDOCK	1	1
HDOCK	0	1
Scorers and Scoring Servers	Top-1	Top-5
Takeda-Shitaka	1***	4/1***/3**
HDOCK	1**	5**
Huang	1**	5**
Kihara	1***	3/1***/2**
HAWKDOCK	1**	5/4**
MDOCKPP	1**	4**
Zou	1**	4**
LZERD	1***	2/1***/1**
Chang	1**	4/3**
Shen	1**	4/3**
Fernandez-Recio	1	3/2**
PYDOCKWEB	1	3/2**
Oliva	1**	2**
Grudin	0	1

Table S2 – Prediction results for Target/Interface T168.1

Predictors	Top-1	Top-5
Zou	1**	5**
Venclovas	1**	5**
Vakser	1**	5**
Seok	1**	5**
Kozakov/Vajda	1**	5**
Kihara	1**	5**
Chang	1**	5**
Bates	1**	5**
Huang	1**	4/3**
Pierce	1**	5/2**
Fernandez-Recio	0	3**
Liwo	1	4
Lubecka	1	3
Czaplewski	1**	1**
CASP-only Predictors	Top-1	Top-5
<i>CoDock</i>	1**	5**
<i>Baker</i>	1**	5/4**
<i>Lamoureux</i>	1**	3**
<i>UNRES</i>	1	4
<i>Takeda-Shitaka</i>	0	1**
Servers	Top-1	Top-5
SWARMDOCK	1**	5**
LZERD	1**	5**
MDOCKPP	1**	5/3**
GALAXYPPDOCK	1**	2**
Scorers and Scoring Servers	Top-1	Top-5
Chang	1**	5**
Oliva	1**	5**
Bonvin	1**	5**
Venclovas	1**	5**
Kihara	1**	5**
Takeda-Shitaka	1**	5**
LZERD	1**	5**
Shen	1**	5**
Zou	1**	5/4**
MDOCKPP	1**	5/4**
HDOCK	1**	4**
Perthold	1	5/3**
Huang	1**	4/3**
SWARMDOCK	1**	3**
Bates	1**	3**
Fernandez-Recio	1**	3**
PYDOCKWEB	1**	3**

Table S2 – Prediction results for Target/Interface T169.1

Predictors	Top-1	Top-5
<i>no acceptable models</i>		
CASP-only Predictors	Top-1	Top-5
<i>no acceptable models</i>		
Servers	Top-1	Top-5
<i>no acceptable models</i>		
Scorers and Scoring Servers	Top-1	Top-5
<i>no acceptable models</i>		

Table S2 – Prediction results for Target/Interface T170.1

Predictors	Top-1	Top-5
Huang	1**	5**
Zou	1	5/1**
Shen	1	5/1**
Venclovas	1	5
Seok	1	5
Kozakov/Vajda	1	5
Fernandez-Recio	1	5
Chang	1	5
Kihara	1	4
Nakamura	1	3
CASP-only Predictors	Top-1	Top-5
<i>Takeda-Shitaka</i>	1	4
<i>DATE</i>	1	2
Servers	Top-1	Top-5
HDOCK	1**	5**
MDOCKPP	1**	5**
CLUSPRO	0	2
Scorers and Scoring Servers	Top-1	Top-5
HDOCK	1**	5/4**
Fernandez-Recio	0	4/3**
PYDOCKWEB	0	4/3**
Huang	1**	5/2**
SWARMDOCK	0	4/2**
Bates	0	4/2**
Zou	1	5/1**
Shen	1	5/1**
Takeda-Shitaka	1	5/1**
MDOCKPP	1	5
Chang	1	5
Venclovas	1	5
LZERD	1	5
Kihara	1	5
Grudin	1	5
Oliva	0	3
Bonvin	1	2

Table S2 – Prediction results for Target/Interface T170.2

Predictors	Top-1	Top-5
Fernandez-Recio	1	5
CASP-only Predictors	Top-1	Top-5
<i>no acceptable models</i>		
Servers	Top-1	Top-5
<i>no acceptable models</i>		
Scorers and Scoring Servers	Top-1	Top-5
<i>no acceptable models</i>		

Table S2 – Prediction results for Target/Interface T170.3

Predictors	Top-1	Top-5
Venclovas	1	5
Seok	1	5
Zou	1	3
Shen	0	3
CASP-only Predictors	Top-1	Top-5
<i>no acceptable models</i>		
Servers	Top-1	Top-5
MDOCKPP	1	5
Scorers and Scoring Servers	Top-1	Top-5
Venclovas	1	4
LZERD	1	3
Chang	1	3
Grudin	0	3
Takeda-Shitaka	1	3
Shen	0	3
Zou	0	2
MDOCKPP	0	2
Oliva	0	1
Kihara	0	1

Table S2 – Prediction results for Target/Interface T170.4

Predictors	Top-1	Top-5
Huang	1	5
Venclovas	0	4
Chang	1	2
CASP-only Predictors	Top-1	Top-5
<i>no acceptable models</i>		
Servers	Top-1	Top-5
HDOCK	1	5
Scorers and Scoring Servers	Top-1	Top-5
HDOCK	1	4
Fernandez-Recio	0	3
PYDOCKWEB	0	3
Venclovas	1	3
Huang	1	2
SWARMDOCK	0	2
Bates	0	2
Chang	0	1
Zou	0	1

Table S2 – Prediction results for Target/Interface T170.5

Predictors	Top-1	Top-5
Shen	1**	5**
Chang	1**	5**
Nakamura	1**	3**
Kozakov/Vajda	1	5/2**
Venclovas	1	5
Seok	1	5
Kihara	1	5
Huang	1	5
Grudinin	1	5
Vakser	1	2
CASP-only Predictors	Top-1	Top-5
<i>DATE</i>	1**	2**
<i>Baker</i>	1	5
<i>VoroCNN-select</i>	1	1
Servers	Top-1	Top-5
CLUSPRO	1	5/1**
HDOCK	1	5
Scorers and Scoring Servers	Top-1	Top-5
Shen	1**	5**
Takeda-Shitaka	1**	5**
Zou	1	4/3**
MDOCKPP	1	5/2**
Chang	1	4/2**
Venclovas	1	5/1**
Fernandez-Recio	1	5/1**
PYDOCKWEB	1	5/1**
Huang	1	5/1**
Grudinin	1	5
HDOCK	1	5
Kihara	1	5
LZERD	1	5
Oliva	0	3/1**
SWARMDOCK	0	4
Bates	0	4

Table S2 – Prediction results for Target/Interface T170.6

Predictors	Top-1	Top-5
Shen	0	1
CASP-only Predictors		
<i>no acceptable models</i>		
Servers		
<i>no acceptable models</i>		
Scorers and Scoring Servers		
Shen	0	1
Takeda-Shitaka	0	1

Table S2 – Prediction results for Target/Interface T170.7

Predictors	Top-1	Top-5
Kihara	1	2
CASP-only Predictors		
<i>no acceptable models</i>		
Servers		
<i>no acceptable models</i>		
Scorers and Scoring Servers		
Kihara	1	2
Oliva	0	1

Table S2 – Prediction results for Target/Interface T170.8

Predictors	Top-1	Top-5
Venclovas	1**	5**
Grudinin	1	5
Chang	1	5
Shen	0	3
Seok	1	3
Kihara	0	2
CASP-only Predictors	Top-1	Top-5
<i>Baker</i>	1**	5/3**
Servers	Top-1	Top-5
LZERD	1	5
Scorers and Scoring Servers	Top-1	Top-5
Venclovas	1**	5/4**
Chang	1	4
Oliva	1	4
Bonvin	1	4
LZERD	1	3
MDOCKPP	0	3
Grudinin	0	3
Zou	0	3
Shen	0	3
Fernandez-Recio	1	2
PYDOCKWEB	1	2
Kihara	0	2
Huang	0	2

Table S2 – Prediction results for Target/Interface T170.9

Predictors	Top-1	Top-5
Shen	0	3
Huang	1	3
Kihara	0	2
Chang	1	2
Seok	1	1
CASP-only Predictors	Top-1	Top-5
<i>Takeda-Shitaka</i>	1	3
Servers	Top-1	Top-5
HDOCK	0	3
Scorers and Scoring Servers	Top-1	Top-5
HDOCK	1	4
Huang	1	3
SWARMDOCK	0	3
Bates	0	3
Shen	0	3
MDOCKPP	0	2
Zou	0	2
Chang	0	2
Grudinin	0	2
LZERD	0	2
Fernandez-Recio	1	1
PYDOCKWEB	1	1
Kihara	0	1

Table S2 – Prediction results for Target/Interface T174.1

Predictors	Top-1	Top-5
<i>no acceptable models</i>		
CASP-only Predictors	Top-1	Top-5
<i>no acceptable models</i>		
Servers	Top-1	Top-5
<i>no acceptable models</i>		
Scorers and Scoring Servers	Top-1	Top-5
<i>no acceptable models</i>		

Table S2 – Prediction results for Target/Interface T176.1

Predictors	Top-1	Top-5
Zou	0	1
Seok	0	1
CASP-only Predictors	Top-1	Top-5
<i>Elofsson</i>	0	1
Servers	Top-1	Top-5
MDOCKPP	0	2
Scorers and Scoring Servers	Top-1	Top-5
Venclovas	0	1
Zou	0	1
MDOCKPP	0	1
Takeda-Shitaka	0	1
SWARMDOCK	0	1
Chang	0	1
Perthold	0	1
Bates	0	1
HAWKDOCK	0	1

Table S2 – Prediction results for Target/Interface T177.1

Predictors	Top-1	Top-5
Zou	1***	5***
Vakser	1***	5***
Pierce	1***	5***
Kozakov/Vajda	1***	5***
Kihara	1***	5***
Huang	1***	5***
Fernandez-Recio	1***	5***
Chang	1***	5***
Bates	1***	5***
Nakamura	1***	4***
Grudin	1***	5/3***/2**
Venclovas	1**	5/2***/3**
Seok	1**	5**
Czaplewski	1**	5**
Liwo	1	5
CASP-only Predictors	Top-1	Top-5
<i>Baker</i>	1***	5***
<i>VoroCNN-select</i>	1***	3***
<i>Lamoureux</i>	1***	2***
<i>DellaCorte</i>	1***	1***
<i>Ornate-select</i>	1**	2**
<i>UNRES</i>	1	5
<i>SBROD</i>	0	1**
<i>ricardo</i>	1**	1**
Servers	Top-1	Top-5
SWARMDOCK	1***	5***
HDOCK	1***	5***
LZERD	1***	5***
MDOCKPP	1***	5***
CLUSPRO	1***	5***
GALAXYPPDOCK	1**	5**
Scorers and Scoring Servers	Top-1	Top-5
SWARMDOCK	1***	5***
Oliva	1***	5***
Bonvin	1***	5***
Bates	1***	5***
HAWKDOCK	1***	5***
Takeda-Shitaka	1***	5***
MDOCKPP	1***	5***
Venclovas	1***	5***
Chang	1***	5/4***/1**
Zou	1***	5/4***/1**
HDOCK	1***	5/4***/1**
Huang	1***	5/4***/1**
PYDOCKWEB	1	5/4***
Shen	1***	4***
LZERD	1***	5/3***/2**
Grudin	1	5/3***
Fernandez-Recio	1**	5**

Table S2 – Prediction results for Target/Interface T177.2

Predictors	Top-1	Top-5
Zou	1***	5***
Venclovas	1***	5***
Vakser	1***	5***
Seok	1***	5***
Pierce	1***	5***
Kozakov/Vajda	1***	5***
Kihara	1***	5***
Huang	1***	5***
Fernandez-Recio	1***	5***
DelCarpio	1***	5***
Chang	1***	5***
Bates	1***	5***
Nakamura	1***	4***
Czaplewski	1***	5/2***/3**
Liwo	1	5
Shen	1**	2/1**
CASP-only Predictors	Top-1	Top-5
<i>Zhang-Assembly</i>	1***	5***
<i>DELCLAB</i>	1***	5***
<i>Baker</i>	1***	5/4***/1**
<i>Lamoureux</i>	1***	2***
<i>Takeda-Shitaka</i>	1***	4/1***/1**
<i>DellaCorte</i>	1**	2/1***/1**
<i>Risoluto</i>	1***	1***
<i>ricardo</i>	1***	1***
<i>UNRES</i>	1	5
<i>VoroCNN-select</i>	0	1**
<i>SBROD</i>	0	1**
<i>Ornate-select</i>	0	1**
Servers	Top-1	Top-5
SWARMDOCK	1***	5***
HDOCK	1***	5***
GALAXYPPDOCK	1***	5***
LZERD	1***	5***
MDOCKPP	1***	5***
CLUSPRO	1***	5***
Scorers and Scoring Servers	Top-1	Top-5
SWARMDOCK	1***	5***
Chang	1***	5***
Oliva	1***	5***
HDOCK	1***	5***
Huang	1***	5***
Bonvin	1***	5***
Bates	1***	5***
LZERD	1***	5***
Zou	1***	5***
MDOCKPP	1***	5***
HAWKDOCK	1***	5***
Takeda-Shitaka	1***	5***
Venclovas	1***	5***
PYDOCKWEB	1	5/4***
Shen	1***	4***
Grudin	1	5/3***
Fernandez-Recio	1***	3/2***
Kihara	1**	3**

Table S2 – Prediction results for Target/Interface T177.3

Predictors	Top-1	Top-5
Venclovas	1**	4**
Zou	1**	4/3**
Grudin	0	3**
Bates	1	5
Kozakov/Vajda	0	2/1**
Pierce	0	1**
Seok	1	2
Nakamura	0	1
Huang	1	1
DelCarpio	1	1
CASP-only Predictors	Top-1	Top-5
<i>VoroCNN-select</i>	0	2**
<i>Ornate-select</i>	1**	1**
<i>Zhang-Assembly</i>	0	2
<i>DellaCorte</i>	1	2
<i>ricardo</i>	1	1
<i>DELCLAB</i>	1	1
<i>Baker</i>	1	1
Servers	Top-1	Top-5
MDOCKPP	1**	5/1***/4**
SWARMDOCK	1	5
CLUSPRO	0	2/1**
HDOCK	1	1
Scorers and Scoring Servers	Top-1	Top-5
SWARMDOCK	1**	5/1***/2**
Bates	1**	5/1***/2**
HAWKDOCK	1**	3/1***/1**
Zou	1**	5/3**
MDOCKPP	1**	4/3**
LZERD	1**	3**
Bonvin	1	3/1**
Fernandez-Recio	1	3/1**
Chang	0	2/1**
Takeda-Shitaka	1**	2/1**
Venclovas	1	4
Oliva	1**	1**
HDOCK	1	2
Huang	1	2

Table S2 – Prediction results for Target/Interface T178.1

Predictors	Top-1	Top-5
Venclovas	1	4/1**
Seok	1	4
Lubecka	1	4
Pierce	1	3
Kihara	0	2
Chang	1	2
Zou	0	1
Liwo	0	1
Fernandez-Recio	0	1
Bates	0	1
CASP-only Predictors	Top-1	Top-5
<i>UNRES.contact</i>	1	4
<i>htjcadd</i>	0	2
<i>CoDock</i>	1	2
<i>Baker</i>	1	2
<i>UNRES</i>	0	1
<i>McGuffin</i>	1	1
Servers	Top-1	Top-5
LZERD	1	2
HAWKDOCK	0	2
MDOCKPP	0	1
Scorers and Scoring Servers	Top-1	Top-5
Takeda-Shitaka	1	5/1**
Chang	1	4/1**
LZERD	1	4
Kihara	0	4
HAWKDOCK	0	2/1**
Venclovas	1	3
MDOCKPP	0	3
Oliva	1	2
Zou	0	2
Shen	0	2

Table S2 – Prediction results for Target/Interface T179.1

Predictors	Top-1	Top-5
Zou	1	4
Venclovas	1	3
Shen	0	2
Liwo	1	2
Chang	0	2
Vakser	0	1
Seok	1	1
Pierce	0	1
CASP-only Predictors	Top-1	Top-5
<i>Baker</i>	1**	1**
<i>UNRES</i>	1	2
<i>CoDock</i>	0	2
Servers	Top-1	Top-5
MDOCKPP	0	1
LZERD	0	1
Scorers and Scoring Servers	Top-1	Top-5
Venclovas	1	3
Fernandez-Recio	1	3
PYDOCKWEB	1	3
MDOCKPP	0	2
Takeda-Shitaka	0	2
Zou	0	2
LZERD	1	2
Kihara	1	2
Grudin	1	2
Bonvin	0	2
Shen	1	2
Chang	0	1
HAWKDOCK	0	1
Oliva	1	1
SWARMDOCK	0	1
Huang	0	1
Bates	0	1

Table S2 – Prediction results for Target/Interface T180.1

Predictors	Top-1	Top-5
Seok	0	1
CASP-only Predictors	Top-1	Top-5
<i>no acceptable models</i>		
Servers	Top-1	Top-5
<i>no acceptable models</i>		
Scorers and Scoring Servers	Top-1	Top-5
PYDOCKWEB	1	1
Venclovas	1	1
Huang	0	1
Fernandez-Recio	0	1

Table S2 – Prediction results for Target/Interface T180.2

Predictors	Top-1	Top-5
Venclovas	1**	5/2***/3**
Kihara	1**	5/1***/4**
Shen	1**	5/4**
Kozakov/Vajda	1**	5/4**
Chang	1**	5/3**
Fernandez-Recio	1**	4/2**
Zou	1	5/1**
Seok	1**	5/1**
Pierce	1**	3/2**
Huang	1**	2**
Lubecka	1	5
Czaplewski	1	5
Liwo	0	4
Vakser	1	1
Grudin	0	1
CASP-only Predictors	Top-1	Top-5
<i>Baker</i>	1	5/4**
<i>CoDock</i>	1**	5/3**
<i>UNRES</i>	1	5
<i>UNRES.contact</i>	1	4
<i>Ornate-select</i>	0	2
<i>VoroCNN-select</i>	0	1
<i>SBROD</i>	0	1
<i>Lamoureux</i>	1	1
Servers	Top-1	Top-5
CLUSPRO	1**	5**
LZERD	1**	4**
GALAXYPPDOCK	1**	1**
MDOCKPP	0	1
Scorers and Scoring Servers	Top-1	Top-5
LZERD	1**	5**
Zou	1**	5**
MDOCKPP	1**	5**
Kihara	1**	5/4**
Huang	1**	5/4**
Chang	1**	5/3**
HDOCK	1**	4/2**
SWARMDOCK	1**	4/1**
Bates	1**	4/1**
Fernandez-Recio	1	4/1**
Venclovas	1	5
Perthold	1	5
Grudin	0	4
Shen	0	2/1**
PYDOCKWEB	1	3
Oliva	1	2
Takeda-Shitaka	0	2

Table S3 – Assembly target performance for T170

Predictors	1	2	3	4	5	6	7	8	9	total
Shen	**	0	*	0	**	*	0	*	*	6/2**
Venclovas	*	0	*	*	*	0	0	**	0	5/1**
Chang	*	0	0	*	**	0	0	*	*	5/1**
Seok	*	0	*	0	*	0	0	*	*	5
Kihara	*	0	0	0	*	0	*	*	*	5
Huang	**	0	0	*	*	0	0	0	*	4/1**
Zou	**	0	*	0	0	0	0	0	0	2/1**
Nakamura	*	0	0	0	**	0	0	0	0	2/1**
Kozakov/Vajda	*	0	0	0	**	0	0	0	0	2/1**
Grudin	0	0	0	0	*	0	0	*	0	2
Fernandez-Recio	*	*	0	0	0	0	0	0	0	2
Vakser	0	0	0	0	*	0	0	0	0	1
CASP-only Predictors										
<i>DATE</i>	*	0	0	0	**	0	0	0	0	2/1**
<i>Baker</i>	0	0	0	0	*	0	0	**	0	2/1**
<i>Takeda-Shitaka</i>	*	0	0	0	0	0	0	0	*	2
<i>VoroCNN-select</i>	0	0	0	0	*	0	0	0	0	1
<i>Kiharalab-assembly</i>	0	0	0	0	0	0	0	*	0	1
Docking Servers										
HDOCK	**	0	0	*	*	0	0	0	*	4/1**
MDOCKPP	**	0	*	0	0	0	0	0	0	2/1**
CLUSPRO	*	0	0	0	**	0	0	0	0	2/1**
LZERD	0	0	0	0	0	0	0	*	0	1
Scorers and Scoring Servers										
Zou	**	0	*	*	**	0	0	*	*	6/2**
Shen	**	0	*	0	**	*	0	*	*	6/2**
Venclovas	*	0	*	*	**	0	0	**	0	5/2**
PYDOCKWEB	**	0	0	*	**	0	0	*	*	5/2**
Huang	**	0	0	*	**	0	0	*	*	5/2**
Fernandez-Recio	**	0	0	*	**	0	0	*	*	5/2**
Chang	*	0	*	*	**	0	0	*	*	6/1**
Takeda-Shitaka	**	0	*	0	**	*	0	0	0	4/2**
Oliva	*	0	*	0	**	0	*	*	0	5/1**
MDOCKPP	*	0	*	0	**	0	0	*	*	5/1**
Kihara	*	0	*	0	*	0	*	*	*	6
SWARMDOCK	**	0	0	*	*	0	0	0	*	4/1**
LZERD	*	0	*	0	*	0	0	*	*	5
HDOCK	**	0	0	*	*	0	0	0	*	4/1**
Grudin	*	0	*	0	*	0	0	*	*	5
Bates	**	0	0	*	*	0	0	0	*	4/1**
Bonvin	*	0	0	0	0	0	0	*	0	2

Table S3 – Assembly target performance for T177

Predictors	1	2	3	total
Zou	***	***	**	3/2***/1**
Venclovas	***	***	**	3/2***/1**
Pierce	***	***	**	3/2***/1**
Kozakov/Vajda	***	***	**	3/2***/1**
Nakamura	***	***	*	3/2***
Huang	***	***	*	3/2***
Bates	***	***	*	3/2***
Vakser	***	***	0	2***
Seok	**	***	*	3/1***/1**
Kihara	***	***	0	2***
Fernandez-Recio	***	***	0	2***
Chang	***	***	0	2***
Grudinin	***	0	**	2/1***/1**
Czaplewski	**	***	0	2/1***/1**
DelCarpio	0	***	*	2/1***
Shen	0	**	0	1/1**
Liwo	*	*	0	2
CASP-only Predictors				
<i>VoroCNN-select</i>	***	**	**	3/1***/2**
<i>DellaCorte</i>	***	***	*	3/2***
<i>Baker</i>	***	***	*	3/2***
<i>ricardo</i>	**	***	*	3/1***/1**
<i>Ornate-select</i>	**	**	**	3/3**
<i>Lamoureux</i>	***	***	0	2***
<i>UNRES</i>	**	***	0	2/1***/1**
<i>Seok-assembly</i>	**	***	0	2/1***/1**
<i>Zhang-Assembly</i>	0	***	*	2/1***
<i>SBROD</i>	**	**	0	2/2**
<i>DELCLAB</i>	0	***	*	2/1***
<i>Takeda-Shitaka</i>	0	***	0	1***
<i>Risoluto</i>	0	***	0	1***
Docking Servers				
MDOCKPP	***	***	***	3***
CLUSPRO	***	***	**	3/2***/1**
SWARMDOCK	***	***	*	3/2***
HDOCK	***	***	*	3/2***
LZERD	***	***	0	2***
GALAXYPPDOCK	**	***	0	2/1***/1**
Scorers and Scoring Servers				
SWARMDOCK	***	***	***	3***
HAWKDOCK	***	***	***	3***
Bates	***	***	***	3***
Zou	***	***	**	3/2***/1**
Takeda-Shitaka	***	***	**	3/2***/1**
Oliva	***	***	**	3/2***/1**
MDOCKPP	***	***	**	3/2***/1**
LZERD	***	***	**	3/2***/1**
Chang	***	***	**	3/2***/1**
Bonvin	***	***	**	3/2***/1**
Venclovas	***	***	*	3/2***
Huang	***	***	*	3/2***
HDOCK	***	***	*	3/2***
Fernandez-Recio	**	***	**	3/1***/2**
Shen	***	***	0	2***
PYDOCKWEB	***	***	0	2***
Grudinin	***	***	0	2***
Kihara	0	**	0	1/1**

Table S3 – Assembly target performance for T180

Predictors	1	2	total
Venclovas	0	***	1***
Seok	*	**	2/1**
Zou	0	**	1/1**
Shen	0	**	1/1**
Pierce	0	**	1/1**
Kozakov/Vajda	0	**	1/1**
Kihara	0	**	1/1**
Huang	0	**	1/1**
Chang	0	**	1/1**
Vakser	0	*	1
Lubecka	0	*	1
Liwo	0	*	1
Fernandez-Recio	0	*	1
CASP-only Predictors			
<i>Seok-assembly</i>	0	**	1/1**
<i>Kiharalab-assembly</i>	0	**	1/1**
<i>CoDock</i>	0	**	1/1**
<i>Baker</i>	0	**	1/1**
<i>UNRES_contact</i>	0	*	1
<i>UNRES</i>	0	*	1
<i>Seok-naive</i>	0	*	1
<i>Lamoureux</i>	0	*	1
Docking Servers			
LZERD	0	**	1/1**
GALAXYPPDOCK	0	**	1/1**
CLUSPRO	0	**	1/1**
Scorers and Scoring Servers			
Huang	*	**	2/1**
Zou	0	**	1/1**
Venclovas	*	*	2
SWARMDOCK	0	**	1/1**
Shen	0	**	1/1**
PYDOCKWEB	*	*	2
MDOCKPP	0	**	1/1**
LZERD	0	**	1/1**
Kihara	0	**	1/1**
HDOCK	0	**	1/1**
Fernandez-Recio	*	*	2
Chang	0	**	1/1**
Bates	0	**	1/1**
Takeda-Shitaka	0	*	1
Perthold	0	*	1
Oliva	0	*	1
Grudin	0	*	1

Table S4 – Complete participant performance

Rank	Predictors	Participation	Top-1	Top-5	Score
1	Seok	14	8/2**	9/4**	13
	Venclovas	14	7/2**	8/1***/3**	13
3	Chang	14	7/2**	8/3**	11
	Zou	14	5/3**	8/3**	11
5	Kihara	14	5/3**	7/3**	10
	Pierce	13	6/3**	7/3**	10
7	Huang	14	5/3**	5/3**	8
	Bates, Kozakov/Vajda	14	4/3**	5/3**	8
	Fernandez-Recio	14	3/2**	5/3**	8
11	Shen	14	3/1**	6/1**	7
	Vakser	14	3**	4/3**	7
13	Nakamura	11	2/1**	3/2**	5
14	Liwo	12	2	3	3
	Czaplewski	13	2/1**	2/1**	3
16	Lubecka	8	2	2	2
	Gray	1	1	1**	2
18	Del Carpio	9	1	1	1
	Grudinin	13	1	1	1
CASP-only Predictors		Participation	Top-1	Top-5	Score
	<i>Baker</i>	14	7/4**	8/1***/3**	13
	<i>CoDock</i>	10	5/1**	6/2**	8
	<i>Takeda-Shitaka</i>	14	2/1**	4/1***/1**	7
	<i>Seok-assembly</i>	14	5/1**	5/1**	6
	<i>Kiharalab-assembly</i>	13	3/1**	5/1**	6
	<i>Lamoureux</i>	11	3**	3**	6
	<i>UNRES</i>	13	2	3	3
	<i>DellaCorte</i>	6	2/1**	2/1**	3
	<i>DATE</i>	11	1	2/1**	3
	<i>Risoluto</i>	14	2	2	2
	<i>Elofsson</i>	13	1	2	2
	<i>htjcadd</i>	6	1	2	2
	<i>AILON</i>	6	1**	1**	2
	<i>ricardo</i>	3	1**	1**	2
	<i>VoroCNN-select</i>	13	1	1**	2
	<i>Ornate-select</i>	10	1	1**	2
	<i>Seok-naive</i>	6	0	1**	2
	<i>SBROD</i>	11	0	1	1
	<i>DELCLAB</i>	9	1	1	1
	<i>McGuffin, UNRES.contact</i>	7	1	1	1
	<i>Zhang-Assembly</i>	5	1	1	1
Rank	Servers	Participation	Top-1	Top-5	Score
1	MDOCKPP	14	4/2**	7/1***/2**	11
2	LZERD	14	4/2**	6/2**	8
3	GALAXYPPDOCK	14	5/1**	5/1**	6
	SWARMDOCK	14	3/2**	4/2**	6
5	HDOCK, CLUSPRO	14	2/1**	3/1**	4
7	HAWKDOCK	6	1	2	2
Rank	Scorers and Scoring Servers	Participation	Top-1	Top-5	Score
1	Zou	14	5/3**	10/3**	13
	Chang	14	6/3**	9/4**	13
	MDOCKPP	14	5/3**	9/4**	13
	Takeda-Shitaka	14	5/1***/2**	8/1***/3**	13
5	Shen	14	5/3**	9/3**	12
	LZERD	14	7/1***/2**	8/1***/2**	12
7	Huang	14	5/4**	7/4**	11
8	Oliva	14	6/3**	7/3**	10
	Fernandez-Recio	14	5/2**	7/3**	10
	PYDOCKWEB	14	5/1**	7/3**	10
	Kihara	14	5/1***/1**	7/1***/1**	10
	Bates, SWARMDOCK	14	4/3**	6/1***/2**	10
	HAWKDOCK	10	3/2**	6/1***/2**	10
15	Venclovas	13	6/2**	7/2**	9
	HDOCK	14	5/3**	5/4**	9
17	Grudinin	14	1	5/1**	6
	Bonvin	14	3/2**	4/2**	6
19	Perthold	9	1	2/1**	3

Table S5 – Interface prediction accuracy

Rank	Name	#correct	#total	#interface	#target	fraction of correct interfaces	Recall		Precision	
							μ	σ	μ	σ
Predictors										
1 -	Huang	30	111	23	12	0.27	48.4%	30%	52.0%	31%
2 -	Liwo	27	100	20	10	0.27	39.1%	31%	32.6%	21%
3 -	Czaplewski	28	105	21	11	0.27	31.1%	30%	38.3%	27%
4 -	Venclovas	28	115	23	12	0.24	55.2%	29%	59.8%	27%
5 -	Kozakov/Vajda	27	115	23	12	0.23	42.9%	29%	54.1%	27%
6 -	Shen	24	109	23	12	0.22	52.5%	27%	52.4%	24%
7 -	Zou	25	115	23	12	0.22	41.2%	31%	56.2%	32%
8 -	Bates	24	115	23	12	0.21	38.3%	32%	45.5%	30%
9 -	Grudin	23	110	22	11	0.21	33.5%	23%	51.4%	30%
10 -	Vakser	18	94	23	12	0.19	45.4%	31%	51.9%	29%
11 -	Kihara	21	115	23	12	0.18	54.9%	27%	50.0%	25%
12 -	Pierce	20	110	22	11	0.18	42.9%	28%	53.9%	26%
13 -	Chang	19	115	23	12	0.17	56.1%	27%	58.0%	26%
14 -	Seok	18	115	23	12	0.16	54.0%	28%	49.2%	26%
15 -	DelCarpio	9	56	12	9	0.16	33.0%	29%	31.9%	26%
16 -	Nakamura	10	73	20	9	0.14	50.9%	29%	54.6%	25%
17 -	Lubecka	6	45	9	8	0.13	42.1%	23%	36.0%	17%
18 -	Fernandez-Recio	12	115	23	12	0.10	35.8%	28%	52.8%	27%
CASP-only Predictors										
1 -	Risoluto	15	54	23	12	0.28	34.4%	26%	37.2%	26%
2 -	Elofsson	8	30	22	11	0.27	40.9%	28%	40.1%	24%
3 -	Seok-assembly	25	95	22	12	0.26	31.4%	27%	30.2%	23%
4 -	UNRES	27	105	21	11	0.26	38.7%	30%	31.6%	21%
5 -	Kiharalab-assembly	22	100	20	11	0.22	36.9%	27%	39.0%	28%
6 -	Ornate-select	14	65	13	10	0.22	36.4%	24%	48.3%	28%
7 -	Lamoureux	10	51	14	11	0.20	50.8%	29%	46.5%	26%
8 -	DATE	10	54	18	9	0.19	47.6%	27%	48.9%	23%
9 -	VoroCNN-select	13	77	21	12	0.17	31.3%	23%	45.0%	30%
10 -	bioinsilico.sbi	5	30	6	6	0.17	21.4%	13%	43.8%	24%
11 -	MULTICOM-AI	7	45	9	7	0.16	33.1%	21%	31.6%	21%
12 -	CoDock	8	55	11	10	0.15	52.8%	26%	51.1%	23%
13 -	UNRES_contact	6	40	8	7	0.15	39.0%	22%	34.2%	17%
14 -	Takeda-Shitaka	14	106	23	12	0.13	46.6%	27%	56.2%	26%
15 -	DELCLAB	7	55	11	9	0.13	33.9%	28%	35.9%	26%
16 -	htjcadd	4	30	6	6	0.13	33.1%	22%	43.4%	20%
17 -	Baker	13	115	23	12	0.11	46.1%	29%	58.1%	27%
18 -	SBROD	8	70	14	11	0.11	32.3%	22%	47.7%	30%
19 -	Seok-naive	3	29	7	6	0.10	33.9%	24%	42.8%	21%
Servers										
1 -	MULTICOM-CLUSTER	23	90	18	12	0.26	24.0%	24%	22.8%	22%
2 -	HDOCK	27	109	23	12	0.25	48.2%	27%	49.2%	30%
3 -	GALAXYPPDOCK	25	104	22	12	0.24	34.8%	30%	33.6%	26%
4 -	LZERD	27	115	23	12	0.23	40.2%	30%	42.5%	30%
5 -	CLUSPRO	20	109	23	12	0.18	45.2%	27%	53.0%	25%
6 -	SWARMDOCK	16	100	20	12	0.16	32.7%	31%	42.4%	31%
7 -	MDOCKPP	17	114	23	12	0.15	38.1%	31%	53.3%	34%
8 -	HAWKDOCK	4	30	6	6	0.13	33.1%	22%	43.4%	20%
Scorers										
1 -	Bonvin	35	115	23	12	0.30	44.3%	29%	43.7%	29%
2 -	Perthold	15	50	10	9	0.30	50.0%	27%	39.8%	22%
3 -	Zou	29	115	23	12	0.25	52.8%	29%	53.0%	26%
4 -	Takeda-Shitaka	24	100	23	12	0.24	56.0%	27%	57.4%	26%
5 -	Huang	27	115	23	12	0.23	57.8%	26%	50.3%	26%
6 -	Venclovas	25	110	22	11	0.23	51.3%	30%	56.5%	29%
7 -	Chang	25	115	23	12	0.22	55.8%	28%	54.7%	26%
8 -	Shen	25	115	23	12	0.22	47.9%	29%	53.0%	26%
9 -	Grudin	22	115	23	12	0.19	45.3%	28%	46.6%	27%
10 -	Fernandez-Recio	21	114	23	12	0.18	51.3%	29%	52.2%	29%
11 -	Oliva	19	115	23	12	0.17	47.1%	28%	50.6%	28%
12 -	Kihara	18	115	23	12	0.16	52.7%	26%	49.3%	26%
13 -	Bates	17	113	23	12	0.15	58.4%	28%	48.3%	26%
Scoring Servers										
1 -	MDOCKPP	29	115	23	12	0.25	57.9%	26%	54.0%	24%
2 -	HDOCK	25	112	23	12	0.22	53.2%	28%	51.9%	28%
3 -	PYDOCKWEB	21	114	23	12	0.18	51.8%	30%	50.8%	28%
4 -	SWARMDOCK	17	113	23	12	0.15	58.4%	28%	48.3%	26%
5 -	LZERD	15	114	23	12	0.13	53.8%	29%	50.8%	27%
6 -	HAWKDOCK	4	60	12	10	0.07	68.4%	24%	56.0%	24%

Table S5 – Interface prediction accuracy. Interface rank based on the fraction of correctly predicted interfaces. Interfaces are defined as correct when both recall and precision values exceed 50%. Recall and precision values are averaged over ligand and receptor entities. Columns list the number of correct interfaces (#correct), the total number of interfaces (#total), and the target (#target) and interface (#interface) participation. μ and σ values are average and standard deviation of recall and precision values over all predicted interfaces.

Extended Abstracts of individual participants

The responsibility for the accuracy of the individual Extended Abstracts lies with the authors of each Abstract.

I. Protein complex assembly by employing particle swarm optimization

Raphael.A.G. Chaleil, Tereza Clarence and **Paul.A.Bates**

*Biomolecular Modelling Laboratory, The Francis Crick Institute, 1 Midland Road, London NW1 1AT, UK
paul.bates@crick.ac.uk*

The construction, optimization and docking of protein models remains challenging. All require extensive sampling of the high dimensional conformational space, which is intractable with methods based on exhaustive enumeration of all possible solutions. Moreover, the exact contributions of the two recognized mechanisms for protein-protein complex formation, ‘conformational selection’ and ‘induced fit’, are not known for any specific interaction. In order to address these problems, we have developed a series of heuristic methods based on Particle Swarm Optimization (PSO).

Methods

Our general methodology for protein fold construction and docking can be described as follows:

i) Fold construction using our automatic server 3D-Jigsaw-SL

The protocol first searches for homologous sequences to the query sequence using HHBlits¹ against a sequence profile database of known structures clustered at 70% sequence identity. A linear *ab initio* polypeptide corresponding to the query sequence is constructed, taking into account the bond lengths, angles and torsion angles accordingly to identified homologous fragments. All the coil regions that are not matched with a structural template are automatically adjusted in torsion angle space. The central core of the algorithm is a constricted PSO², which searches for a minimal Dfire³ statistical pair potential energy. When distance information was available, either from PSICOV⁴ or from discontinuous templates, a Hookean force was applied as a distance restraint mechanism. Two strategies were applied for folding the structures, the first one adjusts all the torsion angles between all the fragments at once, whereas the second one adjusts the torsion of each linker region (i.e., regions between fragments from templates) one at a time, starting from the N-terminal. The latter technique is computationally more expensive; however, it achieves to generate structures with a smaller radius of gyration (i.e., the structures are more globular). This property allows to generate better, i.e., biophysically sound, models. Finally, the top 10 ranking models from 100 replicates of the algorithm at 10000 iterations (according to Dfire) are then minimized with CHARMM⁵ (version 22) and the top structure, identified as having the best CHARMM energy after minimization, is selected for subsequent submission to our protein docking server, SwarmDock. For each section of a protein model different templates might have been chosen; therefore, relating models to single templates is not always possible with this methodology.

ii) Docking using SwarmDock

For the modelling of all protein complexes, we used a modification to our binary protein-docking algorithm SwarmDock⁶. Our method uses the principles of PSO to search the parameter docking space. The innovations added to our automated binary server is, for homo-oligomers, to treat each particle within the swarm as an instance of a packed homo-oligomer, constrained by the appropriate symmetry operators. The objective is to optimize the particle space in order to find the most energetically favourable homo-oligomer. Particles move through a multi-parameter space by the optimization of two sets of parameters: orientations and translations of each monomeric unit relative to the imposed symmetry and linear combinations of normal modes that adjust the conformation of each monomer, in the presence of the other monomers, in this simultaneous docking process. For hetero-oligomeric structures we employed our standard SwarmDock (<https://bmm.crick.ac.uk/~svc-bmm-swarmdock>) protocol⁶. This docking methodology isn't template based. Moreover, additional information, such as potential sequence conservation at the protein-protein interface, was not considered. The ranking of docked poses was obtained using our 'democratic' scoring system, as previously described⁷. To an extent, we considered both the principle of 'conformational selection' and 'induced fit' in our docking procedure. Conformational selection, by using a variety of starting protein conformations⁸, obtained either by our own protein modelling server, *3D-Jigsaw-SL*, or protein models taken from the CASP14 server tar file. Induced fit, is considered too since small adjustments are made in both the backbones and sidechains of the interacting proteins upon docking via the employment of our PSO procedure.

Results

For this round of CASP-CAPRI our results show substantial room for improvement. Only for targets classified as easy (T164, T166, T177), and on one target classified as Difficult (T178, manual model), did the above method show some utility. Interestingly, our manual submissions ranked slightly better than for our server, SwarmDock. This we attribute to having more accurately built models to feed into the docking procedure. For the automated server runs, we didn't have the time to consider alternative input model protein folds to those produced by our fold construction software, *3D-Jigsaw-SL*, a software package in the early stages of development. For the manual submission phase, we were able to test other input model constructs from the CASP14 server tar file. Perhaps not surprisingly, this seems to have made a noticeable difference; the accuracy of the output depends upon the accuracy of the input.

Conclusion

It is not formally a requirement that docking servers in CASP-CAPRI should both build protein folds as well as dock them. However, since success in docking, at least in our hands, requires high quality input models, and high quality protein fold modelling servers around the world tend to have long queues and waiting times, to keep a cutting edge in developing our docking server, our own input models, generated from primary amino acid sequences of the unbound component parts, must be developed to a higher standard; therefore, to facilitate and end-to-end docking methodology, as much time will need to be invested in producing accurate input models as to developing further the actual docking modules.

Availability

Our automated binary protein-protein docking server, SwarmDock, can be located at:

<https://bmm.crick.ac.uk/~svc-bmm-swarmdock/>

References

1. Remmert M., Biegert A., Hauser A. & Söding J. (2011). HHblits: Lightning-fast iterative protein sequence searching by HMM-HMM alignment. *Nat. Methods*. 9(2),173-5.
2. Eberhart, R. C. & Kennedy, J. (1995). A new optimizer using particle swarm theory. In *Proceedings of the sixth international symposium on micro machine and human science* (pp. 39–43), Nagoya, Japan. Piscataway: IEEE.
3. Yang, Y. & Zhou, Y. (2008). Specific interactions for *ab initio* folding of protein terminal regions with secondary structures. *Proteins* 72, 793-803.
4. Jones D.T., Buchan D.W, Cozzetto D & Pontil M. (2012). PSICOV: precise structural contact prediction using sparse inverse covariance estimation on large multiple sequence alignments. *Bioinformatics*. 28(2), 184-90.
5. Brooks B.R., Brooks C.L. 3rd, Mackerell AD Jr, Nilsson L, Petrella RJ, Roux B, Won Y, Archontis G, Bartels C, Boresch S, Caflisch A, Caves L, Cui Q, Dinner A.R., Feig M, Fischer S, Gao J, Hodoscek M, Im W, Kuczera K, Lazaridis T, Ma J, Ovchinnikov V, Paci E, Pastor R.W., Post C.B., Pu J.Z., Schaefer M, Tidor B, Venable RM, Woodcock, H.L., Wu X, Yang W, York, D.M. & Karplus M. (2009). CHARMM: the biomolecular simulation program. *J. Comput. Chem.* 30(10), 1545-614.
6. Torchala M., Moal I.H., Chaleil R.A.G, Fernandez-Recio, J. & Bates P.A.(2013). SwarmDock: a server for flexible protein-protein docking. *Bioinformatics*. 29(6), 807-9.
7. Moal, I., Barradas-Bautista, D., Jimenez-Garcia, B., Torchala, M., van der Velde, A., Vreven, T., Weng, Z., Bates, P.A. & Fernandez-Recio., J. (2017). IRaPPA: information retrieval based integration of biophysical models for protein assembly selection. *Bioinformatics*, 33(12), 1806-1813.
8. Torchala M., Gerguri, T., Chaleil, R.A.G., Gordon, P., Russell, F., Keshani, M. & Bates, P.A. (2020). Enhanced sampling of protein conformational states for dynamic cross-docking within the protein-protein docking server SwarmDock. *Proteins* 88, 962-972.

II. Summary, Chang group, CAPRI Round 50 (CASP14-CAPRI)

Ren Kong, Bin Liu, Guangbo Yang, Ming Liu, Hang Shi, Xufeng Lu, Shan Chang*

Institute of Bioinformatics and Medical Engineering, School of Electrical and Information Engineering, Jiangsu University of Technology, Changzhou 213001, China. E-mail: schang@jsut.edu.cn

In CASP14-CAPRI, our group combined template-based modeling and *ab-initio* docking protocol as hybrid docking strategy called CoDock [1, 2] for the docking and scoring experiments. For each target, we queried Protein Data Bank (PDB) for structures of protein homologs that can be used as template for modeling the homo and hetero protein complexes. The templates for each target are listed in Table 1. If no proper template was available, we used the *ab-initio* docking protocol to perform the global searching, such as T172 and T173. For T170, we partly modeled the hetero 15-mer complex according to the template 6J0N and applied *ab-initio* docking to obtain the final structure of the hetero 27-mer complex. Then, two different binding modes are submitted by our group, as shown in Figure 1.

A knowledge-based scoring function was trained based on the statistical mechanics-based iterative method [3] and used in CoDock program. This knowledge-based scoring function included much more information of near-native structures in the observed pair distribution function, enabling it more robust for conformational changes. Since the scorer results for all targets in Round 50 are evaluated by CAPRI, we summarized our performance in Table 1. For T165, T169 and T174, no group obtained acceptable models. For T167, T175 and T181, there are no evaluated data provided by CAPRI. The 3 targets of T171-173 are canceled by CASP. Only 9 targets have available data for analysis. For 8 targets of T164, T166, T168, T170, T176, T177, T178, and T179, our docking protocol achieved acceptable quality or better models in the scoring competitions. Our group failed mainly in the target of T180. The minimum number of subunits of T180 may not be chosen correctly in our submissions.

Table 1. List of templates and scoring performance of our group (S3) for each target

CAPRI ID (CASP ID)	Template	Stochiometry	Scoring performance of Top-5 ^a
T164 (T1032) ^b	1GXL, 6OIS	A2	*
<i>T165 (H1036)</i> ^c	5ZS0, 4OT1, 5C6T	A3B3C3	--
T166 (H1045)	2Y9M, 4BWF, 5NKZ	A1B1	**
T167 (T1050)	4A2L, 3V9F, 4A2M, 3OTT, 3VA6	A2	No data
T168 (T1052)	6F7D, 6F7K	A3	**
<i>T169 (T1054)</i>	4QO6, 2OBV, 4ODJ	A2	--
T170 (H1060)	6J0N	A6B3C12D6	*
T171(T1063)	2MVW, 6QAJ	A4	Canceled
T172 (H1066)	-- ^d	A1B1	Canceled
T173 (H1069)	--	A1B1	Canceled
<i>T174 (T1070)</i>	1S2E, 5IV5, 5IV7, 1QEX	A3	--
T175 (T1073)	4G6Q	A4	No data
T176 (T1078)	3V0R	A2	*
T177(H1081)	2VYC, 5XX1	A20	**
T178 (T1083)	1U4Q, 3GWK, 5MTO, 5ME8	A2	**
T179 (T1087)	3GWK, 5LOS	A2	*
T180(T1099)	3J2V, 6HTX	The minimum number of subunits	--
T181 (H1103)	6XDC	A1B1	No data
Total			8/4**

^a ‘***’ and ‘*’ indicate medium and acceptable quality models achieved by our group, respectively. ‘--’ represents no acceptable models obtained by our group. ‘No data’ represents no evaluated data provided by CAPRI. ‘Canceled’ represents the target canceled by CASP.

^b In these 8 targets, our group achieved acceptable or better models in scoring experiments.

^c No groups obtained acceptable models in T165, T169 and T174.

^d No proper template was available for T172 and T173.

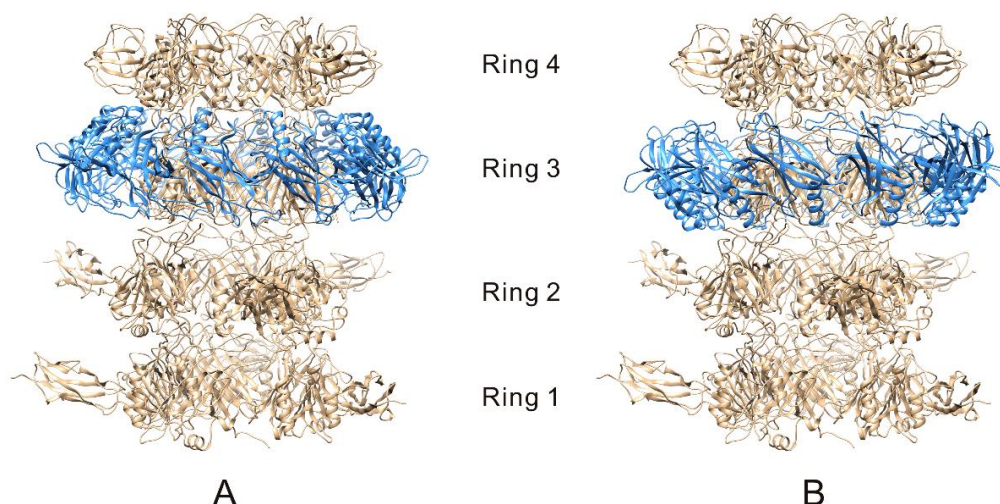


Figure 1. Two different binding modes of T170 are predicted by the *ab-initio* docking of CoDock. The hetero 15-mer is colored brown and the homo 12-mer is colored blue.

References:

- [1] Kong R, Wang F, Zhang J, Xu X J, Chang S. CoDockPP: a multistage approach for global and site-specific protein-protein docking. *J Chem Inf Model.* 2019; 59(8): 3556-3564.
- [2] Kong R, Liu R R, Xu X M, Zhang D W, Xu X S, Shi H, Chang S. Template-based modeling and *ab-initio* docking using CoDock in CAPRI. *Proteins.* 2020; 88(8): 1100-1109.
- [3] Huang S-Y, Zou X. An iterative knowledge-based scoring function for protein-protein recognition. *Proteins.* 2008; 72(2): 557-579.

III. Reconstructing Protein Complex Structure from Predicted Inter-Chain Contacts in CAPRI-Round50

Raj S. Roy, Farhan Quadir, Jian Liu and Jianlin Cheng
 Department of Electrical Engineering and Computer Science, University of Missouri, Columbia, MO 65211, USA

Our MULTICOM-AI protein complex structure predictor uses *ab initio* deep learning-based interchain contact prediction tool (DNCON2_Inter¹) as well as a template-based prediction method (TBP) to predict interchain contacts for complex targets in CASP14 and CAPRI50. The predicted inter-chain contacts are then used to create the quaternary structure of the target by a custom distance-geometry protocol based on Crystallography & NMR System (CNS)².

Availability: https://github.com/jianlin-cheng/DNCON2_Inter

Methods

The individual sequences and predicted (“known”) tertiary structures of the subunits of a target protein complex are given to the MULTICOM-AI system as input. Its prediction workflow is illustrated in **Figure 1**.

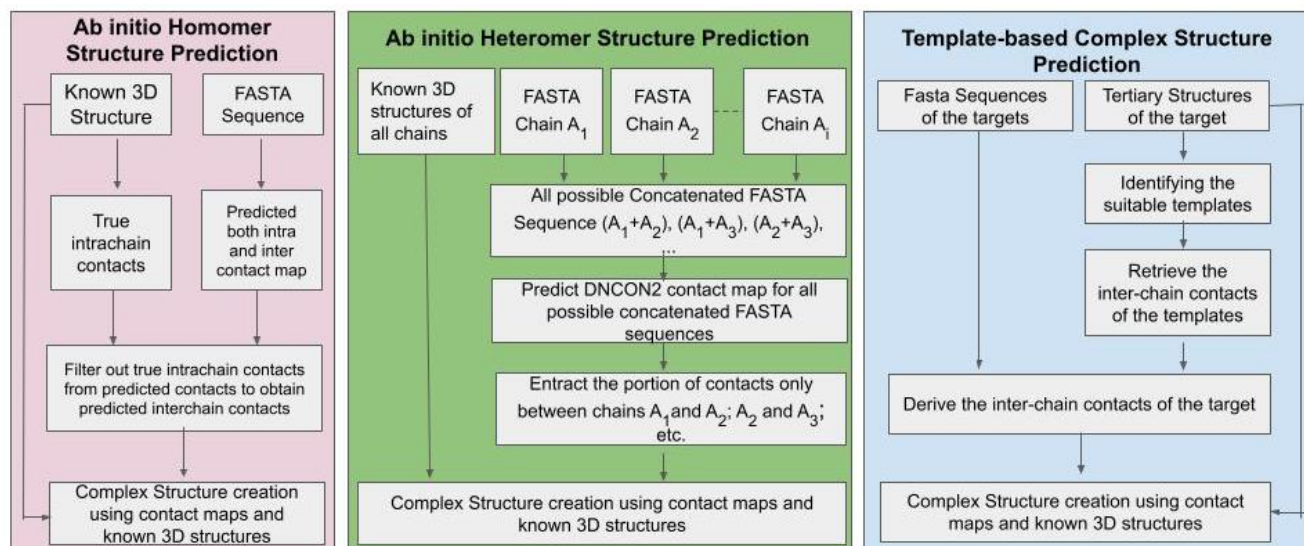


Figure 1: The workflow of the MULTICOM-AI complex structure prediction system. The box on the left illustrates the deep learning prediction of inter-chain contacts for homodimers, the box in the middle the deep learning prediction of inter-chain contacts for heterodimers, and the box on the right the template-based prediction of inter-chain contacts. The predicted contacts are used to generate the quaternary structure of a dimer. Interchain residue pairs are considered interchain contacts if the Euclidean distance between the two closest heavy atoms of the two residues is $\leq 6.0 \text{ \AA}^{1,4}$.

Interchain Contact Prediction. The pairs of chains in a complex are treated as dimers - homodimer if two chains are identical and heterodimer otherwise. Since the multiple sequence alignment (MSA) of a monomer in a homodimer is essentially the same as that of the homodimer itself, the deep learning-based contact predictor (DNCON2_Inter) using the MSA of a monomer in a homodimer as input predicts both interchain and intrachain contacts³. The intra-chain contacts are then filtered out according to the “known” tertiary structure of the monomer to keep interchain contacts only (pink box in Figure 1). The tertiary structure is predicted by MULTICOM⁴. The process for heterodimer contact prediction is slightly different (green box in Figure 1). We concatenate the individual sequences of the two chains and generate MSA for heterodimers by searching the combined sequence against a custom database of concatenated sequences of interacting dimers derived from the Protein Data Bank (PDB). It is then fed to our deep learning predictor to generate the interchain contact map. For TBP (blue box in Figure 1), we search the tertiary structures of the protein chains against the custom dimer structure database to find complex templates and then extract the interchain contacts from them. The tertiary structures of individual chains and the predicted interchain contact maps are then fed to the complex structure construction system based on CNS to generate the final structures of the complex as follows.

Inter-Chain Contact-Guided Complex Structure Generation. The method is implemented on top of the distance geometry protocol of CNS, which uses a stochastic simulated annealing method to build the complex structure of protein dimers, leveraging predicted interchain protein contacts and tertiary structures of individual protein chains. It can build complex structures consisting of two or more protein chains, keeping the individual protein chains unchanged and trying to satisfy inter-chain contacts as well as possible. It generates 100 models, which are then sorted in the ascending order of the distance-restrain energy. The top 5 models with minimum energy are selected.

Results

Table 1 shows the precision of the inter-chain contact prediction for a good example - Target T164. It is a homodimer, where each chain contains 284 residues. Figures 2 (A) and (B) depict the contact map predicted by DNCON2_Inter and TBP in comparison with the true contact map, respectively.

Table 1: The precision of top k contact predictions by DNCON2_Inter and TBP for T164, where $k = \{5, 10, L/10, \dots, 2L\}$ and L: length of protein sequence.

Method	Precision (%)						
	Top 5	Top 10	Top L/10	Top L/5	Top L/2	Top L	Top 2L
Dncon2_Inter	100	100	100	100	52.8	26.4	13.2
TBP	100	100	100	100	100	54.6	27.3

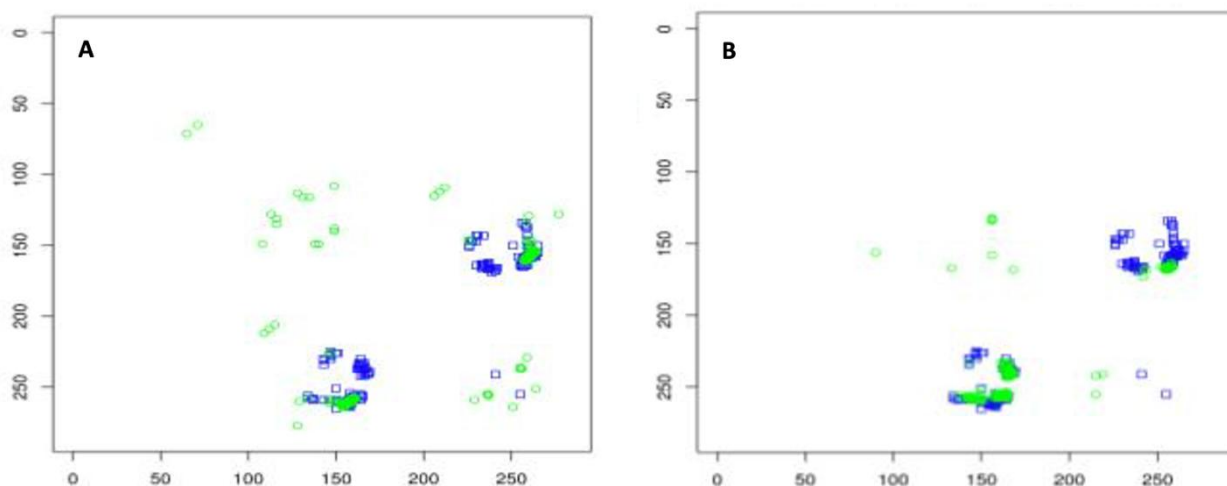


Figure 2: (A) Inter-chain contacts predicted by DNCON2_Inter (green) versus true contacts (blue); (B) Inter-chain contacts predicted by TBP (green) versus true contacts (blue).

Acknowledgements

This work is supported in part by Department of Energy grants (DE-AR0001213, DE-SC0021303, and DE-SC0020400), NSF grants (DBI 1759934 and IIS1763246), and an NIH grant (R01GM093123).

References

1. Quadir, F., Roy, R., Halfmann, R., & Cheng, J. DNCON2_Inter: Predicting interchain contacts for homodimeric and homomultimeric protein complexes using multiple sequence alignments of monomers and deep learning. Research Square; 2021. DOI: 10.21203/rs.3.rs-228041/v1.
2. Brunger, A. T. (2007). Version 1.2 of the Crystallography and NMR system. *Nature protocols*, 2(11), 2728.
3. Liu, J., Wu, T., Guo, Z., Hou, J., & Cheng, J. Improving protein tertiary structure prediction by deep learning and distance prediction in CASP14. *bioRxiv*, 2021.
4. Hopf, T. A., Schärfe, C. P., Rodrigues, J. P., Green, A. G., Kohlbacher, O., Sander, C., ... & Marks, D. S. (2014). Sequence co-evolution gives 3D contacts and structures of protein complexes. *Elife*, 3, e03430.

IV. Extended Abstract: UNRES group

A. Antoniak,¹ C. Czaplewski,¹ A. Giełdoń,¹ M. Kogut,¹ A.G. Lipska,¹ A. Liwo,¹ E.A. Lubecka,² M. Maszota-Zieleniak,¹ A.K. Sieradzan,¹ R. Ślusarz,¹ P.A. Wesółowski,^{1,3} K. Zięba¹

¹Faculty of Chemistry, University of Gdańsk, Wita Stwosza 63, 80-308 Gdańsk, Poland,

²Faculty of Electronics, Telecommunications and Informatics, Gdańsk University of Technology, G. Narutowicza 11/12, 80-233 Gdańsk, Poland,

³Intercollegiate Faculty of Biotechnology, University of Gdańsk and Medical University of Gdańsk, ul. Abrahama

58, 80-307 Gdańsk, Poland

We participated in CAPRI Round 50 as three groups: UNRES (group 55; 22 predictions), UNRES-contact (group 53; 12 predictions), and UNRES-template (group 04; 22 predictions), respectively, all of which used the latest version of the coarse-grained UNRES force field [1]. The UNRES group used plain UNRES force field with only weak restraints on secondary structure [2] obtained from PSIPRED, the UNRES-contact group used contact prediction accomplished by using the DNCON2 method [3] or extracted from server models, while the UNRES-template group used distance- and local-structure restraints extracted from server models, as described previously [4]. The restraints were imposed only on monomers. The UNRES software was modified to handle large oligomeric targets.

The protocol for oligomer-structure prediction. Initial multimeric models were built from monomer structures. The monomers were, in turn, modeled, within the CASP14 experiment, by using our hierarchical protocol, in which restrained MREMD (Multiplexed Replica Exchange Molecular Dynamics) [5] simulations with the coarse-grained UNRES force field [1] were carried out. Simulations of monomers were started from multiple server models.

Targets 177 (CASP14 target H1081) and 180 (CASP14 target T1099) were special cases. The initial 20-mer of target 177 was obtained as two stacked rings of the experimental decamer (PDB: 3n75), rotated with respect to each other structure to avoid overlaps. The initial structure of target 180 was built using symmetry constraints from the i-TASSER model of monomer selected to avoid overlaps, for which purpose the C-terminal part of each oligomer had to be regenerated, subject to symmetry constraints. Whole structure of this target was simulated, while the minimal asymmetric unit was submitted.

When good oligomer templates were available (as found by HHpred [6]), the initial structures of oligomers were modeled on template scaffold, while in other cases the monomers were assembled into the initial oligomer structures by using the random-oligomer-positioning algorithm of UNRES-dock [7]. For each target, multiple oligomer structures were constructed. The starting structures were subjected to restrained MREMD simulations with the UNRES force field [1], as described previously [2,4]. Subsequently, simulation results were processed by using the Weighted Histogram Analysis Method (WHAM) [8] and cluster analysis to extract 10 families of conformations [2,4]. The families are ranked based on their free energies (each computed over the entire conformational sub-ensemble constituting a family [1]). Coarse-grained structures which were closest to the cluster centers were subsequently converted to all-atom representation by using the PULCHRA [9] and SCWRL [10] knowledge-based algorithms, and subjected to final refinement at the all-atom level with the AMBER ff14SB force field [11].

Results

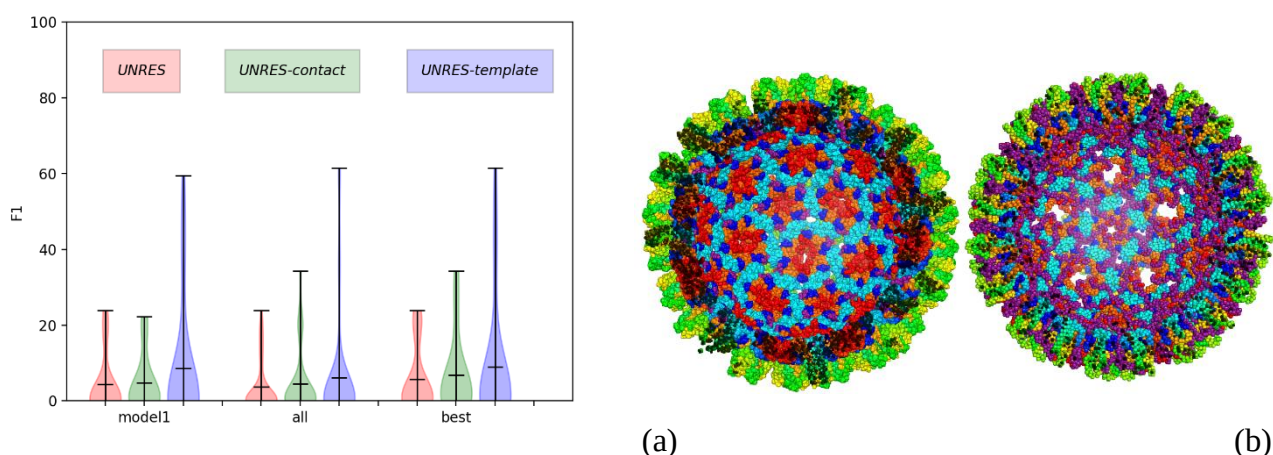


Figure 1. (a) Violin plots of the distributions of the F1 measure of fitting the modeled structures to the experimental structures of the targets treated by the three UNRES-based groups. (b) The experimental 2vgh structure of the duck hepatitis virus capsid (target 180) (left) and the structure modeled by UNRES (right).

As shown from Figure 1a, including knowledge-based restraints on monomers results in much better quality of the best models; however its influence on the average F1 value is less significant.

In our experience [4], round 50 was more difficult compared to the previous rounds of CAPRI because of lesser availability of good templates for the oligomers and because of significantly greater size of the targets.

Acknowledgments

Supported by National Science Center of Poland (Narodowe Centrum Nauki) (NCN), grants UMO-2017/25/B/ST4/01026, UMO-2017/26/M/ST4/00044, and UMO-2017/27/B/ST4/00926. Computational resources were provided by (a) the Interdisciplinary Centre of Mathematical and Computational Modelling (ICM) at the University of Warsaw (b) the Centre of Informatics – Tricity Academic Supercomputer & Network (CI TASK) in Gdańsk, (c) the Polish Grid Infrastructure (PL-GRID), and (d) our Beowulf cluster at the Faculty of Chemistry, University of Gdańsk.

- [1] A. Liwo, A.K. Sieradzan, A.G. Lipska, C. Czaplewski, I. Joung, W. Żmudzińska, A. Hałabis, A., S. Ołdziej. *J. Chem. Phys.*, 150 (2019) 155104.
- [2] E.A. Lubecka, A.S. Karczyńska, A.G. Lipska, A.K. Sieradzan, K. Zięba, C. Sikorska, U. Uciechowska, S.A. Samsonov, P. Krupa, M.A. Mozolewska, Ł. Golon, A. Giełdoń, C. Czaplewski, R. Ślusarz, M. Ślusarz, S.N. Crivelli, A. Liwo. *J. Mol. Graph. Model.* 92 (2019) 154-166.
- [3] B. Adhikari, J. Hou, J. Cheng. *Bioinformatics* 34 (2018) 1466-1472.
- [4] A.S. Karczyńska, K. Zięba, U. Uciechowska, M.A. Mozolewska, P. Krupa, E.A. Lubecka, A.G. Lipska, C. Sikorska, S.A. Samsonov, A.K. Sieradzan, A. Giełdoń, A. Liwo, R. Ślusarz, M. Ślusarz, J. Lee, K. Joo, C. Czaplewski. *J. Chem. Inf. Model.*, 60 (2020) 1844-1864.
- [5] Y.M. Rhee, V.S. Pande, *Biophys. J.* 84 (2003) 775-786.
- [6] Zimmermann L, Stephens A, Nam SZ, Rau D, Kübler J, Lozajic M, Gabler F, Söding J, Lupas AN, Alva V. *J Mol Biol.* 430 (2018) 2237-2243.
- [7] P. Krupa, A.S. Karczyńska, M.A. Mozolewska, A. Liwo, C. Czaplewski. *Bioinformatics*, (2021) btaa897, <https://doi.org/10.1093/bioinformatics/btaa897>
- [8] S. Kumar, D. Bouzida, R.H. Swendsen, P.A. Kollman, J.M. Rosenberg. *J. Comput. Chem.* 13 (1992) 1011-1021.
- [9] P. Rotkiewicz, J. Skolnick. *J. Comput. Chem.* 29 (2008) 1460-1465.
- [10] Q. Wang, A.A. Canutescu, R.L. Dunbrack. *Nat. Protoc.* 3 (2008) 1832-1847.
- [11] J.A. Maier, C. Martinez, K. Kasavajhala, L. Wickstrom, K.E. Hauser and C. Simmerling. *J. Chem. Theory Comput.* 11, (2015) 3696-3713.

V. INCORPORATING FLEXIBILITY BY SOFT DOCKING IN MIAx

Carlos A. Del Carpio Muñoz^{1*}, Eiichiro Ichiishi²

¹Nagoya City University, Graduate School of Medical Sciences, Kawasumi, Mizuho-cho, Mizuho-ku, Nagoya, 467-8601 Japan

²International University of Health and Welfare Hospital (IUHW Hospital) 537 Iguchi, Nasushiobara-city, Tochigi Pref. 329-2763, Japan

Introduction:

Incorporating flexibility in protein docking algorithms has become a key issue in computational methodologies oriented to solve the protein-protein interaction (PPI) prediction problem in molecular biology. Backbone rearrangement and, to a larger extent, amino acid side chain rearrangement shape the interacting subunits at the interface of the complex, post-docking re-modeling of the interfaces being required when rigid docking algorithms are applied to solve the PPI problem for unbound subunits. The difficulty arises in predicting and scoring high the best decoys (closest to the native structure), the interfaces of which may undergo extensive rearrangement at interaction. Here we propose a genuine methodology to undertake this problem that consists in an a-priori treatment of the molecules to dock that combines a softening technique of the surface of the molecules, and the utilization of graph morphological operations to deal with protein flexibility resulting in a new concept of “soft docking” that mainly targets the docking of unbound protein molecules (reported at the isolated state).

The methodology is embedded as an independent module into our system for macromolecular interaction assessment system MIAx (Macromolecular Interaction Assessment Computer System)^{1,2,3}, that has been in continuous development for the last decade. Results of applying the newly proposed soft docking technique to the set of benchmark protein complexes reported in the literature illustrate its ability to generate close-to-native decoys even before re-modeling the interaction interfaces.

Methodology:

The key strategy is the mapping of a characteristic shape from the unbound conformation for the protein by applying a three dimensional filter to the function representing the surface. The high flexibility of the amino acids on the molecular surface can be expressed introducing in this way “softness” in the rigid docking algorithm, allowing some unrealistic penetrations among the interacting proteins that may lead to better prediction of the complex configuration. Moreover, the elimination of the atomistic detail of the molecular surface by replacing it with a smoother function enables the treatment of the protein as a three dimensional graph, to which morphological operations can be applied in order to accentuate or smooth protuberances or grooves on the surface that may play the main roles in the interaction process. This allows the manipulation of flexible docking in a way mimicking induced fit in PPI.

Results and Discussion:

If only the geometrical features of the interacting monomers are used to dock the structures, the system performs well for a set of difficult docking problems. We show, thus, that a priori knowledge on the binding sites or the automatic identification of binding regions on the surfaces of the interacting macromolecules can substantially improve the ranking of the decoys output by the rigid body docking of the unbound proteins. Moreover, a refinement of the structures can be performed to deal with the most flexible chains in the interacting interface of the best decoys. The optimization process would be confined to a relatively small section of the conformational space as we have shown in previous reports about flexible docking; the algorithm constitutes therefore a powerful tool to predict those starting conformations. Nonetheless, since more and more structures resulting from large scale genome sequencing projects may have to be modeled rather than determined by experimental methods, containing therefore several significant structural errors, methodologies like the one presented here may prove of great assistance in structure-based functional studies requiring

computational techniques with the capacity of docking large number of protein models within acceptable limits of accuracy as our methodology does before the refinement process by flexible docking. Indeed, the methodology proposed here was validated with monomers that in several cases are not 100% similar in amino acid sequence, the effectiveness of the methodology having been proven and the results are described in a paper under publication.

References.

1. Del Carpio C.A., Ichiishi E., Yoshimori A., Yoshikawa T.; "MIAX: A New Paradigm to Model Bio-Molecular Interaction and Complex Formation in Condensed Phases"; *PROTEINS: Structure, Function and Genetics*, 48(4) (2002), 696-732
 2. Del Carpio C.A., Campbell W., Constantinescu I., Gyongyossy-Issa M.I.C., "Rational design of antithrombotic peptides to target the von Willebrand Factor (vWf) - GPIIb integrin interaction"; *J. Mol. Modeling* (2008) 14:1191-1202
- Del Carpio C. A., Ichiishi E.,(2017) "Inference of protein multimeric complex dynamic order of formation: an active region recognition based approach." *Int. J. Genom. Data Min: IJGD-116*. DOI: 10.29011/IJGD-116. 000016

VI. Rosetta docking strategies in the CASP14-CAPRI experiment

Ameya Harmalkar, Jeffrey J. Gray

Chemical and Biomolecular Engineering, Johns Hopkins University, Baltimore, MD, USA

Introduction

Performance of docking methods in prior CAPRI challenges have revealed that the intrinsic flexibility of proteins still hampers the accuracy of docking predictions¹. In this edition of CASP14-CAPRI, we expanded and evaluated our docking methods in Rosetta to tackle the binding-induced conformational flexibility in protein-protein docking. To model the targets in this round, we employed our recent progress in RosettaDock² and SymDock³; along with our upcoming replica-exchange method, ReplicaDock 2.0 (built upon work from Zhang, Schindler, Lange and Zacharias^{4,5}), that utilizes induced-fit with docking.

Model Curation

From the given amino acid sequence, we used the BLAST program to identify homologous proteins. Based on the availability of a suitable template, we determined the three-dimensional structure of a target or the monomer with MODELLER⁶. If no template was available, we built models using the Robetta web server. For antibody targets such as T165, modeling the complementarity-determining region is challenging as it is less conserved. In order to improve our predictions with antibody targets, we employed RosettaAntibody⁷ and DeepH3⁸ developed by our group.

Docking Methods

Rigid-docking for identification of binding sites: To obtain putative binding sites, we performed ab-initio docking using rigid-body Fast Fourier Transform (FFT) based docking using the ClusPro⁹ web server. We also performed rigid-body global sampling using our ReplicaDock protocol and clustered the lowest energy decoys. As both of these tools generate multiple bound structures, we compared the ligand root mean square deviations (L_rmsd) and chose those poses that had the ligand in same relative neighborhood for local docking. By using this pipeline, we were able to narrow down the global search into a local search, where it was feasible to sample conformational changes near putative binding regions.

RosettaDock 4.0: Our recent work on protein docking uses a conformer-selection based Monte Carlo Minimization (MCM) approach. Starting from a putative binding region obtained

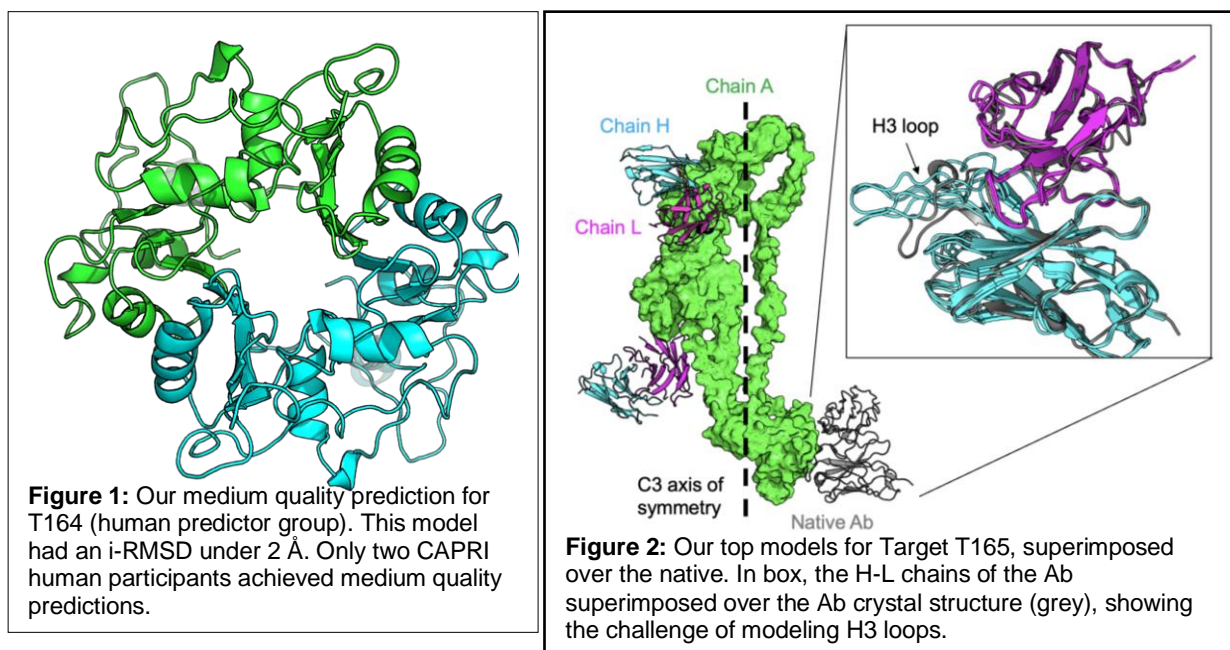
post global search, we dock the targets using our RosettaDock 4.0 protocol that adaptively swaps receptor and ligand conformers from a pre-generated ensemble of structures in the coarse-grained stage followed by an all-atom refinement in the high-resolution stage. To diversify the backbone conformations in the ensemble, we generate structures using Rosetta Relax, backbone flexing with Backrub¹⁰ and normal-modes. Further, we use an updated coarse-grained energy function i.e. Motif Dock Score (MDS)² obtained from 6-dimensional residue pair data to efficiently discriminate non-native decoys from native ones.

ReplicaDock 2.0: We recently developed a new, aggressive conformational sampling methodology incorporating temperature and Hamiltonian-replica exchange Monte Carlo (T-REMC⁴ and H-REMC⁵) techniques coupled with the induced-fit (IF) mechanism of protein binding. By capturing backbone motions of putative interface residues on-the-fly, we mimic the partner-specific moves of IF approaches within our docking protocol. This approach communicates between multiple replicas with different energy functions and temperatures to better explore the backbone conformational space. For this CASP14-CAPRI round, we first performed a global docking with the replica exchange protocol restricting motion to only rigid body moves to sample the protein energy landscape. Upon narrowing down putative local binding sites, we performed replica exchange docking with IF-backbone motion. We initiated 8 trajectories of the docking simulation, each trajectory spanning over 3 temperature replicas, run for 2.5×10^5 MC steps. With inverse temperatures set to β , of 1.5^{-1} kcal⁻¹.mol, 3^{-1} kcal⁻¹.mol and 5^{-1} kcal⁻¹.mol, replica exchange swaps are attempted every 1000 MC steps generating 6,000 decoys at a local binding site.

SymDock 2.0: To navigate the challenges pertaining to targets with point symmetries, we utilize the symmetry framework in our docking protocol SymDock2³. We dock monomer chains related by a symmetry-axis. The use of a new scoring function (MDS) and an all-atom backbone flexibility in the high-resolution stage allows us to obtain tighter interface packing for symmetric targets, and in turn improve the quality of our predictions. This is reflected in our medium quality targets obtained for target T164, a symmetric homo-dimer with C2 symmetry.

Successes and Failures

We participated in 2 targets of the CASP14-CAPRI blind prediction experiment. For target T164 (Fig. 1), we were one of the only two groups that generated medium-quality predictions (and multiple acceptable-quality predictions). This was particularly interesting as we fused the SymDock2 ensembles with monomer chains obtained from the ReplicaDock2 IF-based docking approach. The method of induced-fit outperformed other methods, perhaps by capturing putative native-like conformations in the presence of the partner. For target T165 (Fig. 2) which involved a glycoprotein-antibody complex with C3 symmetry, like all other groups we were unable to obtain acceptable predictions. The failure in modeling target T165 stems from the limitations in our ability to accurately model the H3 loop of the antibody.



References

1. Harmalkar, A. & Gray, J. J. Advances to tackle backbone flexibility in protein docking. *Curr. Opin. Struct. Biol.* **67**, 178–186 (2020).
2. Marze, N. A., Roy Burman, S. S., Sheffler, W. & Gray, J. J. Efficient flexible backbone protein-protein docking for challenging targets. *Bioinformatics* **34**, 3461–3469 (2018).
3. Roy Burman, S. S., Yovanno, R. A. & Gray, J. J. Flexible Backbone Assembly and Refinement of Symmetrical Homomeric Complexes. *Structure* **27**, 1041-1051.e8 (2019).
4. Zhang, Z. & Lange, O. F. Replica Exchange Improves Sampling in Low-Resolution Docking Stage of RosettaDock. *PLoS One* **8**, e72096 (2013).
5. Zhang, Z., Schindler, C. E. M., Lange, O. F. & Zacharias, M. Application of Enhanced Sampling Monte Carlo Methods for High-Resolution Protein-Protein Docking in Rosetta. *PLoS One* **10**, e0125941 (2015).
6. Webb, B. & Sali, A. Comparative Protein Structure Modeling Using MODELLER. *Curr. Protoc. Bioinforma.* **54**, 5.6.1-5.6.37 (2016).
7. Weitzner, B. D., Jeliakov, J. R., Lyskov, S., Marze, N., Kuroda, D., Frick, R., Adolf-Bryfogle, J., Biswas, N., Dunbrack, R. L. & Gray, J. J. Modeling and docking of antibody structures with Rosetta. *Nat. Protoc.* **12**, (2017).
8. Ruffolo, J. A., Guerra, C., Mahajan, S. P., Sulam, J. & Gray, J. J. Geometric potentials from deep learning improve prediction of CDR H3 loop structures. *Bioinformatics* **36**, i268–i275 (2020).
9. Kozakov, D., Hall, D. R., Xia, B., Porter, K. A., Padhorny, D., Yueh, C., Beglov, D. & Vajda, S. The ClusPro web server for protein-protein docking. *Nat. Protoc.* **12**, 255–278 (2017).
10. Smith, C. A. & Kortemme, T. Backrub-like backbone simulation recapitulates natural protein conformational variability and improves mutant side-chain prediction. *J. Mol. Biol.* **380**, 742–756 (2008).

VII. HADDOCK scoring of CAPRI Round50 models.

Bonvin A.M.J.J.^{1*}, Ambrosetti F., Honorato R.V., Jandova Z., Jiménez-García B. Koukos P.I., van Keulen S., van Noort C., Réau M., Roel-Touris J.

Computational Structural Biology Group, Bijvoet Centre for Biomolecular Research, Department of Chemistry, Faculty of Science, Utrecht University, 3584CH, Utrecht, The Netherlands.

* To whom correspondence should be addressed: a.m.j.j.bonvin@uu.nl

Scoring methodology

The HADDOCK team only participated as scorers in this CASP/CAPRI round. The scoring was purely based on energetics considerations, not making use of any experimental and/or bioinformatics information such as conservation or co-evolution. In this section, we describe the followed scoring pipeline, consisting of the following steps:

1) Pre-processing of models. This initial step consists of identifying possible problematic models (e.g., cases with missing chains, missing atoms, etc) and correcting for amino-acid nomenclature (e.g., renaming HSD/HSE, AMBER nomenclature, to HIS).

2) Short energy minimisation. Each model is subjected to a short energy minimisation using HADDOCK2.4¹ (<https://www.bonvinlab.org/software/haddock2.4>). For each model, any missing atoms (but not missing segments) are built, the protonation state of histidines is automatically set by comparing the electrostatic energies of the various histidine states (charged or neutral with the proton attached to either the N or E nitrogen atom on the ring) and disulphide bridges are automatically detected based on a distance cut-off. Once all missing atoms have been built, the model is subjected to 50 steps of energy minimisation with the OPLS forcefield² with a non-bonded cutoff of 8.5Å.

3) Scoring. The energy minimized models generated by the last step are scored with the simple HADDOCK scoring function (HS)³, which is a linear weighted sum of energetic and structural terms:

$$HS_{it} = 1.0 E_{vdw} + 0.2 E_{ele} + 1.0 E_{deso}$$

where E_{vdw} , E_{ele} and E_{deso} stand for van der Waals, Coulomb electrostatics and desolvation energies, respectively. The non-bonded components of the score (E_{vdw} , E_{ele}) were calculated with the OPLS forcefield². The desolvation energy is a solvent accessible surface area-dependent empirical term⁴, which estimates the energetic gain or penalty of burying specific sidechains upon complex formation.

4) Clustering. Despite the possible heterogeneity in model numbering, we perform a clustering of all models based on the fraction of common contacts⁵ using a 0.65 cutoff. Two different clusterings are performed requiring a minimum of 4 and 2 models per cluster, respectively.

5) Cluster-based scoring. For each cluster we calculate an average score based on the top 2 or top 4 models. Clusters are then ranked based on their average HADDOCK score.

6) Model selection. Depending on the degree of clustering, the final selection of models is based either on cluster statistics obtained with a minimum of 2 or 4 models per cluster. A short visual inspection of the cluster is done to exclude “suspect models”. Those are often models scoring much better than any other models, which upon visual inspection appear to be unrealistic models with highly intertwined chains and optimized energetics. Although the origin of the models is unknown to us, we venture to speculate that those most likely originate from fold and dock approaches. The final submission consists of 1 model per cluster for the top5 re-scored set, and depending on the scoring statistic, more models from the top cluster might be included in positions 6 to 10, or models from new clusters are included.

Scoring performance

Table 1 summarises our scoring results for the 12 targets that were assessed, for a total of 23 different interfaces (with T170, T177 and T180 assessed as nine, three and two different interfaces respectively). Overall, we got acceptable or better models for 11 of the 23 interfaces (48%) in the top 10 predictions, which drops to 8 (35%) and 7 (30%) for the top5 and top1, respectively. Note that in our scoring procedures all interfaces are considered simultaneously, and we do not score per interface.

We generally observe that our short minimisation strategy is unable to refine strongly clashing models which end up with very high positive scores. Such models often originate from rigid body docking approaches and might well contain good predictions when it comes to the backbone orientations. Due to their potential high clash content at the interfaces, those models are however severely penalized by our energy-based scoring procedure. Further, comparing our results with others, while we do identify acceptable models for close to 50% of the interfaces in the top10 (the best groups reach ~64% in this round), there is room for improvement since our top5 and top1 performance is dropping. A more aggressive refinement might be needed to further remove clashes and improve the scoring of models together potentially with a re-optimisation of our scoring function.

Table1 – HADDOCK scoring performance per interface. The stars indicate the quality of the selected models and the number before those the number of models of a given quality (*: acceptable; **: medium; ***: high) based on CAPRI criteria.

TARGET/INTERFACE	TOP1	TOP5	TOP10
T164	1*	5*	9*
T165	-	-	-
T166	-	-	1**
T168	1**	5**	10**

T169	-	-	-
T170/1	1*	2*	5*
T170/2-7	-	-	-
T170/8	1*	4*	7*
T170/9	-	-	1*
T174	-	-	-
T176	-	-	-
T177/1	1***	5***	10***
T177/2	1***	5***	10***
T177/3	1*	2*/1**	2*/2**
T178	-	-	2*
T179	-	2*	3*
T180/1	-	-	-
T180/2	-	-	-
OVERALL	4*/1**/2***	4*/3**/2***	6*/3**/2***

Funding

This work was supported by the European H2020 e-Infrastructure grants BioExcel (Grant No. 675728 and 823830), EOSC-hub (Grant No. 777536) and from the Dutch Foundation for Scientific Research (NWO) (TOP-PUNT Grant 718.015.001).

Conflict of interest

Dr. A.M.J.J. Bonvin is a member of the CAPRI management committee but has no access to target information.

References

1. Dominguez C, Boelens R, Bonvin AMJJ. HADDOCK: A Protein–Protein Docking Approach Based on Biochemical or Biophysical Information. *J Am Chem Soc.* 2003;125(7):1731-1737.
2. Jorgensen WL, Tirado-Rives J. The OPLS [optimized potentials for liquid simulations] potential functions for proteins, energy minimizations for crystals of cyclic peptides and crambin. *J Am Chem Soc.* 1988;110(6):1657-1666.
3. Vangone A, Rodrigues JPGLM, Xue LC, et al. Sense and simplicity in HADDOCK scoring: Lessons from CASP-CAPRI round 1. *Proteins Struct Funct Bioinforma.* 2017;85(3):417-423.
4. Fernández-Recio J, Totrov M, Abagyan R. Identification of protein-protein interaction sites from docking energy landscapes. *J Mol Biol.* 2004;335(3):843-865.
5. Rodrigues J.P.G.L.M., Trellet M., Schmitz C., Kastritis P.L., Karaca E., Melquiond A.S.J. and Bonvin A.M.J.J. Clustering biomolecular complexes by residue contacts similarity. *Proteins: Struc. Funct. & Bioinformatic.* 2021;80:1810-1817.

VIII. Hybrid ClusPro approach in 2020 CASP-CAPRI round: template-assisted docking and docking of protein models

Sergei Kotelnikov^{1,2,3}, Dzmitry Padhorny^{1,2}, Kathryn A. Porter⁴, Andrey Alekseenko^{1,2,5}, Mikhail Ignatov^{1,2}, Israel Desta⁴, Ryota Ashizawa^{1,2}, Zhuyezi Sun⁴, Usman Ghani⁴, Nasser Hashemi⁴, **Sandor Vajda^{4,6}**, and **Dima Kozakov^{1,2}**

¹*Department of Applied Mathematics and Statistics, Stony Brook University, Stony Brook, New York*

²*Laufer Center for Physical and Quantitative Biology, Stony Brook University, Stony Brook, New York*

³*Innopolis University, Innopolis, Russia*

⁴*Department of Biomedical Engineering, Boston University, Boston, Massachusetts*

⁵*Institute of Computer-Aided Design of the Russian Academy of Sciences, Moscow, Russia*

⁶*Department of Chemistry, Boston University, Boston, Massachusetts*

In the latest joint CASP-CAPRI assembly round our group used two modeling methods, one of them being a template-based method recently updated and implemented as a fully automated public server ClusPro TBM^{1,2} (tbm.cluspro.org) and the other being the original ClusPro³⁻⁶ server (cluspro.bu.edu) that performs rigid-body docking. Here we briefly describe the basic features of these protocols and present some of the applications and performance highlights.

Methods

Model Preparation

Given the sequences and expected stoichiometry of the target protein complex, we search for available templates in the pdb100 database using HHsearch⁷ and identify those that contain homologs of the interacting biological unit to be predicted (it is also possible to use manually pre-selected templates as input). If no template of the complex is found, we perform free docking using ClusPro. Since free docking requires three-dimensional structures as input, we use the HHpred^{8,9} top template to build a homology model of the subunits using Modeller^{10,11}. Unaligned regions of the target sequence are removed to avoid the addition of unstructured loops and tails into the model, while aligned portions of the target are built with fixed backbone atoms. In difficult cases, we build an “ab initio” model of the subunit using TrRosetta¹².

Template-based docking

Once potential templates containing homologs for all subunits have been identified, the method performs a stoichiometry check, testing whether the template can accommodate the required number of copies of each subunit type. This includes some nontrivial cases like the use of homomeric templates for heteromeric targets or the use of single-chain templates for multimers. If a template of the biological complex satisfying the required stoichiometry is found then we choose the best template for each unique subunit of the complex, align multiple copies of this subunit template to the complex template and then model the whole complex of full-sequence chains using Modeller. In order to diversify the pool of models, we also used the CASP server models of the subunits by aligning those onto our initial template-based models and minimizing the resulting structures. To remove structural redundancy in the final set of resulting assembly models we calculate C α RMSD

between all pairs of models taking into account complex stoichiometry and symmetry (there might be several ways to align the chains of one model onto the other, the minimal RMSD is calculated) and perform greedy clustering at 10 Å radius. Finally, we report the centers of up to 10 largest clusters ranked by the cluster size.

Free Docking

Our free docking protocol starts from running PIPER¹³ - a global rigid-body docking program that performs a systematic search of protein complex conformations on a grid using the fast Fourier transform (FFT). It represents the energy score as a sum of correlation terms that includes vdW interaction energy, electrostatic energy, and desolvation energy contributions calculated by a DARS¹⁴ structure-based statistical pairwise potential. The docking run can be additionally informed by XL-MS cross-links¹⁵ and SAXS data^{16,17} that helps to guide and restrain the search. The top 1000 lowest energy docked complex conformations generated by PIPER are used to compute a matrix of pairwise ligand interface C α RMSD values. Namely, for each docked conformation, we select ligand residues with at least one atom within 10 Å of receptor and calculate C α RMSD for these residues against the remaining 999 ligand poses. Using this not necessarily symmetric matrix as a distance measure we perform greedy clustering of the poses with a clustering radius of 9 Å. After removing potential side chain clashes by fixed backbone minimization of CHARMM¹⁸ vdW energy, we report the centers of the 10 largest clusters as predictions. They are ranked by the cluster size.

Results

Performance highlights

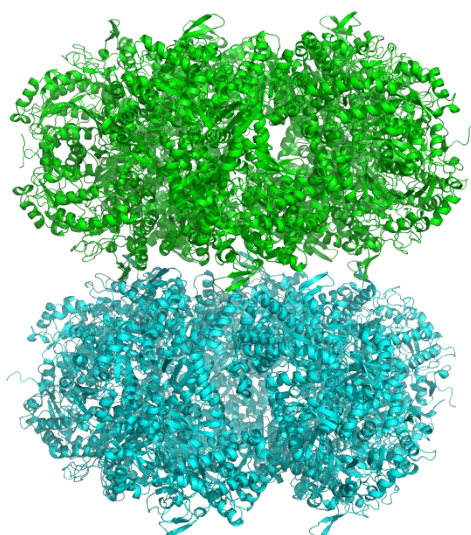


Figure 1. A model of CASP-CAPRI target H1081/T177 generated by a combined TBM/free docking approach. The two identical partial assemblies of A10 stoichiometry modeled with ClusProTBM (shown in green and cyan) were docked to each other using free docking ClusPro capabilities to produce a near-native model.

As mentioned above, in CAPRI/CASP14 we used both template-based and free modeling approaches. A particularly interesting case in which the two methodologies needed to be combined was CASP-CAPRI target H1081/T177, representing a homomultimer of A20 stoichiometry. Here, we found no reasonable template for the whole assembly, and thus a

straightforward TBM approach was not a way forward. However, templates for partial (A10) assembly were abundantly available.

We, therefore, modeled an A10 subcomponent of the target using ClusproTBM based on available templates and then docked two copies of this partial model using the free docking functionality of the ClusPro server. This approach thus represented a synthesis of the two methodologies and resulted in a near-native model of the full target assembly as a result (see Fig. 1).

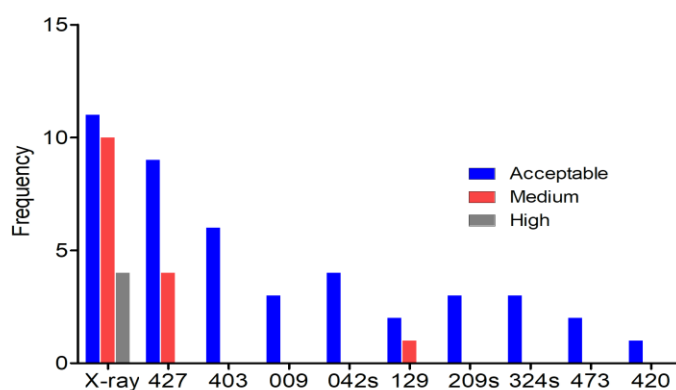


Figure 2. Comparison of free docking results for a set of CASP14 multimeric cases using models generated by top CASP14 predictors as inputs. For each group, the number of acceptable or better predictions in top-5 is given. Docking results obtained by re-docking the subunits taken from the X-ray structure of the complex are provided as a baseline.

Another observation we make in CASP/CASP14 is how the improvement in the quality of folding models leads to a dramatic improvement in the quality of free docking results. When using subunit models produced by the top-performing CASP14 groups as inputs to free docking, the number of modeled interfaces with acceptable or better quality (as estimated by DockQ¹⁹) is comparable to those obtained by re-docking subunits taken from the X-ray structures. Fig. 2 provides the summary of docking results for a set of CASP14 multimeric targets.

Encountered difficulties

Despite the progress in the development of scoring functions, template-based modeling of protein assemblies generally outperforms free docking when good templates are available. However, working with some of the CASP-CAPRI targets demonstrated that even in presence of good but remotely homologous templates, modeling quality might be significantly affected by the quality of sequence alignment, especially in key regions such as complex interfaces.

References

1. Porter, K. A. *et al.* Template-based modeling by ClusPro in CASP13 and the potential for using co-evolutionary information in docking. *Proteins* **87**, 1241–1248 (2019).
2. Padhorny, D. *et al.* ClusPro in rounds 38 to 45 of CAPRI: Toward combining template-based methods with free docking. *Proteins* **88**, 1082–1090 (2020).
3. Desta, I. T., Porter, K. A., Xia, B., Kozakov, D. & Vajda, S. Performance and Its Limits in Rigid Body Protein-Protein Docking. *Structure* **28**, 1071–1081.e3 (2020).

4. Vajda, S. *et al.* New additions to the ClusPro server motivated by CAPRI. *Proteins* **85**, 435–444 (2017).
5. Kozakov, D. *et al.* The ClusPro web server for protein-protein docking. *Nat. Protoc.* **12**, 255–278 (2017).
6. Kozakov, D. *et al.* How good is automated protein docking? *Proteins* **81**, 2159–2166 (2013).
7. Steinegger, M. *et al.* HH-suite3 for fast remote homology detection and deep protein annotation. *BMC Bioinformatics* **20**, 473 (2019).
8. Zimmermann, L. *et al.* A Completely Reimplemented MPI Bioinformatics Toolkit with a New HHpred Server at its Core. *J. Mol. Biol.* **430**, 2237–2243 (2018).
9. Gabler, F. *et al.* Protein Sequence Analysis Using the MPI Bioinformatics Toolkit. *Curr. Protoc. Bioinformatics* **72**, e108 (2020).
10. Webb, B. & Sali, A. Comparative Protein Structure Modeling Using MODELLER. *Curr. Protoc. Protein Sci.* **86**, 2.9.1–2.9.37 (2016).
11. Sali, A. & Blundell, T. L. Comparative protein modelling by satisfaction of spatial restraints. *J. Mol. Biol.* **234**, 779–815 (1993).
12. Yang, J. *et al.* Improved protein structure prediction using predicted interresidue orientations. *Proc. Natl. Acad. Sci. U. S. A.* **117**, 1496–1503 (2020).
13. Kozakov, D., Brenke, R., Comeau, S. R. & Vajda, S. PIPER: An FFT-based protein docking program with pairwise potentials. *Proteins: Structure, Function, and Bioinformatics* vol. 65 392–406 (2006).
14. Chuang, G.-Y., Kozakov, D., Brenke, R., Comeau, S. R. & Vajda, S. DARS (Decoys As the Reference State) potentials for protein-protein docking. *Biophys. J.* **95**, 4217–4227 (2008).
15. Xia, B., Vajda, S. & Kozakov, D. Accounting for pairwise distance restraints in FFT-based protein-protein docking. *Bioinformatics* **32**, 3342–3344 (2016).
16. Ignatov, M., Kazennov, A. & Kozakov, D. ClusPro FMFT-SAXS: Ultra-fast Filtering Using Small-Angle X-ray Scattering Data in Protein Docking. *J. Mol. Biol.* **430**, 2249–2255 (2018).
17. Xia, B. *et al.* Accounting for observed small angle X-ray scattering profile in the protein-protein docking server ClusPro. *J. Comput. Chem.* **36**, 1568–1572 (2015).
18. Brooks, B. R. *et al.* CHARMM: the biomolecular simulation program. *J. Comput. Chem.* **30**, 1545–1614 (2009).
19. Basu, S. & Wallner, B. DockQ: A Quality Measure for Protein-Protein Docking Models. *PLoS One* **11**, e0161879 (2016).

IX. Fernandez-Recio's group performance in CASP14 / CAPRI round 50

Mireia Rosell,^{1,2} Luis A. Rodríguez-Lumbreras,^{1,2} and Juan Fernandez-Recio^{1,2}

¹*Instituto de Ciencias de la Vida y del Vino (ICVV), CSIC - Universidad de La Rioja - Gobierno de La Rioja, Logroño, Spain*

²*Barcelona Supercomputing Center (BSC), Barcelona, Spain*

We have participated as human predictors, human scorers, and server scorers, in all the 12 evaluated targets, comprising a total of 14 assessed interfaces. We applied a similar strategy to that in the CASP13-CAPRI experiment, combining *ab initio* docking, template-based modeling, and energy-based scoring [1].

Methods

The models of the individual subunits were taken from the best predictions of ZHANG, RaptorX, and QUARK CASP-hosted servers, except for target T170, which had available structures for two of the subunits (see Results).

We applied our pyDock [2] docking pipeline to the models of the individual subunits, in order to build the binary interactions in each assembly. In homo-oligomers, only docking poses satisfying the expected symmetry (e.g. cyclic C₂ symmetry for homo-dimers; C₃ for homo-trimers) were selected. For that, rotation angles and translation distances along the

symmetry axis between two docked subunits were calculated by ICM-Browser (www.molsoft.com) as previously described [3]. A given docking pair was defined as C_2 or C_3 symmetry when rotation angle was $180^\circ \pm 5^\circ$ or $120^\circ \pm 1^\circ$, respectively, and translation along symmetry axis $< 5 \text{ \AA}$.

Additionally, we searched for available templates for the assembly interfaces, using BLAST as well as the top five released predictions from the ZHANG, QUARK, RaptorX, MULTICOM-CONSTRUCT and ROSETTA CASP-hosted servers. The models for the individual subunits were superimposed on each template (template-based docking) and minimized with AMBER 12. In targets T165 and T177, some interfaces were modelled with MODELLERv9.19 (template-based modeling) because there were not available models at the CASP-hosted servers (see Results).

Finally, all the (*ab initio* or template-based) modelled interfaces were scored with pyDock. The number of available templates and their reliability determined the proportion of template-based complex models included in the set of submitted models. We eliminated redundant predictions and minimized the top ten submitted models.

In the scorers experiment, we first removed models with more than 250 clashes (i.e., intermolecular pairs of atoms closer than 3 \AA). Then, we scored the models with pyDock (or pyDockWEB [4] as servers) and applied the same additional criteria as in predictors (i.e. in case of reliable templates we favored models similar to such templates, we checked for symmetry, we applied *ad-hoc* distance restraints for specific targets, etc., more details in the Results section). As human scorers we introduced more manual intervention than as server scorers, i.e., removing loops with non-realistic conformations, and re-scoring some of these models afterwards.

Results

In targets for which we could not find available templates (T169, T174, T178, T179), we applied our automatic pyDock docking and scoring pipeline as predictors, and the built-in scoring function of pyDock or pyDockWEB as human or server scorers, respectively, selecting only symmetric orientations (C_2 in T169, T178 and T179; C_3 in T174). We got acceptable results in two of these difficult targets, T178 (as predictors) and T179 (both as human and as server scorers). For the two failing targets, no other participant group was successful.

For the rest of targets, we could find potentially suitable templates for all or some of the predicted interfaces. In most of these cases, we generated models by *ab initio* docking and by template-based modeling independently, and the final proportion of models derived from these two approaches was determined by pyDock scoring and/or by the reliability of the available templates. Thus, *ab initio* docking was favored in target T176, with unsuccessful results (indeed, this was a difficult case, with few successful participants). In target T164, we also favoured *ab initio* docking, since we incorrectly focused on the potential dimerization of the helices. As a consequence, we had unsuccessful results as predictors, but got acceptable models as human and server scores. On the other side, template-based modeling was favored in targets T166, and T168, for which we got medium-quality models as predictors, human scorers and server scorers. Finally, only template-based modeling was applied in target T180, consisting in the assembly of a virus capsid with icosahedral symmetry. We modelled a homo-tetramer, as the minimal number of subunits necessary to define the unique interfaces, and got acceptable results (averaged over the two evaluated interfaces) as predictors, human scorers and server scorers (together with Venclovas, our server scorers were the only acceptable rank 1 submissions of all participants for this target).

In the most challenging multi-molecular targets, in order to build the full assembly we combined template-based docking for some interfaces and *ab initio* docking for the other ones. This is the case of the homo-20mer T177, in which the homo-decamer was modelled with MODELLERv9.19 based on available templates, followed by pyDock scoring, and the final assembly was built by docking two decamers. For this target, we obtained medium-quality results (averaged over the 3 interfaces) as predictors, human scorers and server scorers. In the hetero-nonameric target T165, the homo-trimeric glycoprotein was modelled by template-based docking (i.e. superimposing the subunit models from the CASP-hosted servers on the available templates), and the hetero-dimeric antibody was modelled with MODELLERv9.19 because there were not available models at the CASP-hosted servers. Then, they were docked to form the evaluated hetero-trimeric interface. However, we got unsuccessful results, as the rest of participants.

In the same line, target T170 was a challenging hetero-27mer, in which we applied an *ad-hoc* modeling procedure, also combining *ab initio* docking and template-based modeling. This assembly was formed by three rings with different composition and stoichiometry. The first ring was a homo-hexamer arranged as a dimer of trimers (A3:A3) and was modelled by manually fitting (Figure 1) the monomeric x-ray structure (PDB 5NGJ, chain A) into the available cryo-EM map of bacteriophage T5 tail (EMDB ID: 3689) [5] (trimers built by *ab initio* docking did not fit well into the cryo-EM map). In the final hexameric ring, residues 3-5 and 216-220 were removed due to steric clashes between rings. Interestingly, in the evaluated interface #2 (A3:A3) we submitted the only acceptable model among all participants, as predictors. The second ring was formed by three subunits of one protein and twelve subunits of a second protein (B3:C12) and was modelled by a combination of *ab initio* docking, symmetry restraints, and template-based docking. The third homo-hexameric ring (D6) was modelled by superimposing the x-ray structure of the monomer (PDB 4JMQ) on available templates (PDB 4DIV and 2X8K), followed by minimization and pyDock scoring (Figure 1). The final assembly of the modelled rings was done by *ab initio* docking, selecting only models in which the symmetry axes of the rings were aligned. The same criteria was used in the scorers experiment. The different interfaces in this target were evaluated in three separate groups. In the average evaluation over interfaces #1 (A3), #2 (A3:A3), #3 (B3) and #4 (A3:B3), we got unsuccessful results (despite having acceptable models for interfaces #1 and #2 as predictors). In the averaged evaluation over interfaces #5 (C12), #6 (B3:C12) and #7 (B3:C12), we also got unsuccessful results. However, in the averaged evaluation for interfaces 8 (D6) and 9 (B3:D6), we obtained acceptable results as human and server scorers (together with Venclovas, these were the only acceptable rank 1 submissions of all participants).

In summary, our results for the modeling of multi-meric assemblies in CASP14 were in line with those in the past CASP13-CAPRI edition. Interestingly, our performance as human predictors, human scorers, and human servers has been quite consistent, and in the majority of cases our successful predictions were achieved with our rank 1 submissions, which is an improvement with respect to past editions. However, in the interfaces without suitable template or experimental information we had significantly worse predictions, which shows that *ab initio* docking of multi-meric assemblies is far from being solved.

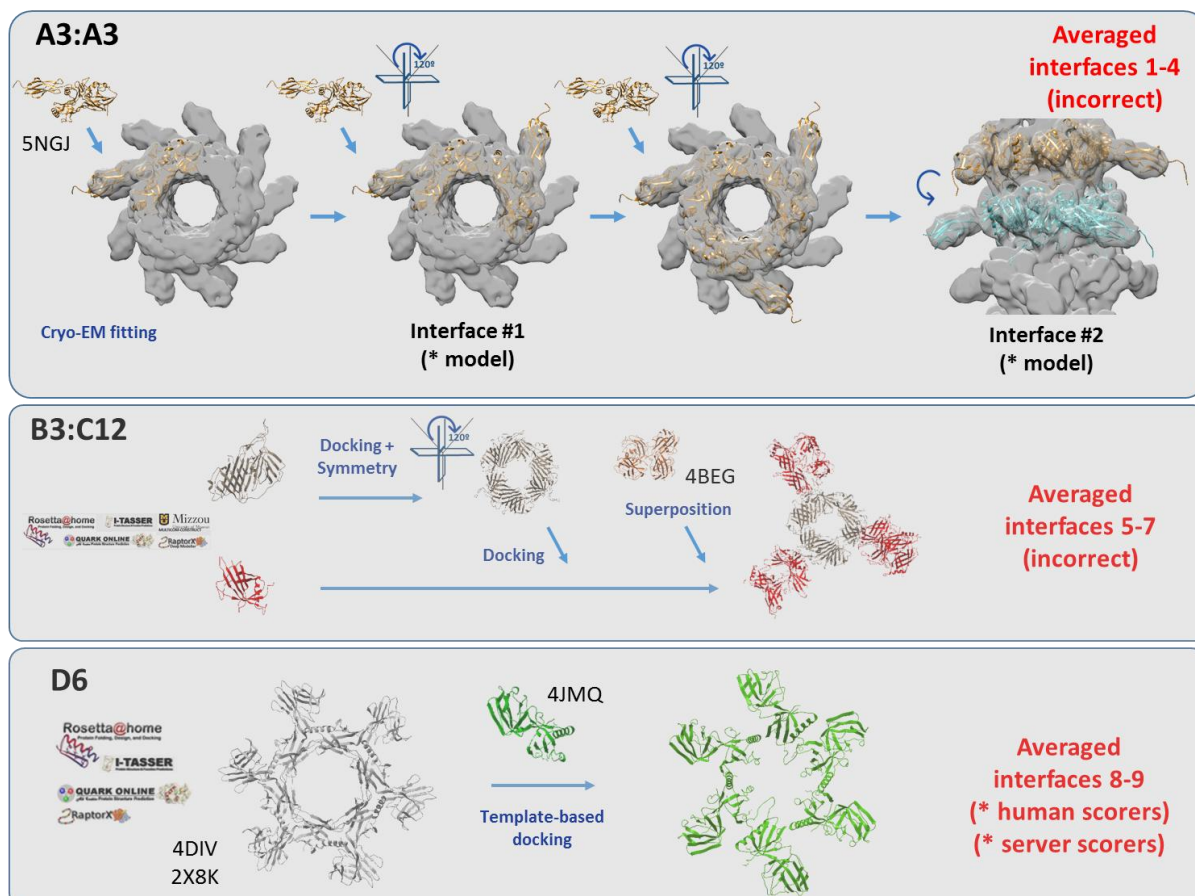


Figure 1. Modeling strategies for the three major rings in target T170.

- [1] Lensink, M.F., Brysbaert, G., Nadzirin, N., et al. (2019). Blind prediction of homo- and hetero-protein complexes: The CASP13-CAPRI experiment. *Proteins*. **87**, 1200-1221.
- [2] Cheng, T.M.-K., Blundell, T.L. & Fernandez-Recio, J. pyDock: electrostatics and desolvation for effective scoring of rigid-body protein-protein docking. *Proteins* **68**, 503–515 (2007).
- [3] Rosell, M., Rodríguez-Lumbreras, L.A., & Fernandez-Recio, J. (2020) Modeling of Protein Complexes and Molecular Assemblies with pyDock. *Methods Mol. Biol.* **2165**, 175-198.
- [4] Jimenez-Garcia, B., Pons, C. & Fernandez-Recio, J. (2013) pyDockWEB: a web server for rigid-body protein-protein docking using electrostatics and desolvation scoring. *Bioinformatics*. **29**, 1698-1699.
- [5] Arnaud, C.A., Effantin, G., Vivès, C., Engilberge, S., Bacia, M., Boulanger, P., Girard, E., Guy Schoehn, G. & Breyton, C. (2017) Bacteriophage T5 tail tube structure suggests a trigger mechanism for Siphoviridae DNA ejection. *Nature Comm.* **8**, 1953.

X. Quaternary structure prediction using a combination of physics-based approaches with machine learning

Agnieszka Karczynska and Sergei Grudin

Univ. Grenoble Alpes, Inria, CNRS, Grenoble INP, LJK, 38000 Grenoble, France
 agnieszka.karczynska@inria.fr, sergei.grudin@inria.fr

In the CAPRI round 50, we combined rigid-body free docking with several quality assessment (QA) methods developed in our lab. We extensively used the symmetry assembler SAM⁴ and the binary docking method Hex⁵. Some targets also motivated us to develop novel methods. For example, we extended SAM⁴ symmetry assembler for helical symmetries, we introduced new options into the symmetry analyzer AnAnaS^{10,11}, we developed a novel rigid-body replica-exchange Markov-chain Monte Carlo simulation technique, we introduced symmetry constraints into the interactive docking engine¹², and more.

Methods:

Prediction round:

Firstly, we selected best-scored CASP14 stage-2 server predictions according to QA methods developed in our lab: VoroCNN¹, VoroCNN-sh⁸, Ornate², and SBROD³. Next, we used them as initial monomeric models for molecular docking. For each target, we used around 40 initial monomeric models. For the homo-oligomeric targets, we ran SAM⁴ on each model, specifying the desired symmetry. For the hetero-dimers, we performed cross-docking using the Hex program. We generated from 5,000 to 20,000 docking poses, depending on the size of the target, and then we scored them using our QA methods. Finally, we submitted the best assembly predictions based on the competition rank. More precisely, for each of the models, we computed *weighted interface scores* as $S_{\text{interface}} = (S_{AB} * N_{AB} - S_A * N_A - S_B * N_B) / N_{AB}$, where S_{AB} is a QA score of the multimeric model, N_{AB} is the number of residues in the multimeric model, S_A and S_B are the individual QA scores of the assembly components A and B, and N_A and N_B are the corresponding numbers of residues. We then ranked all the interfaces by the standard competition ranking. We repeated this procedure for each QA method. The 100 assembly models with the highest number of summed up ranking points were submitted to CAPRI as our predictions.

Scoring round:

For the scoring round, we calculated scores using our QA methods for each provided complex model and its subunits. Then, we computed the interface score for each model and rank them according to the standard competition ranking described above.

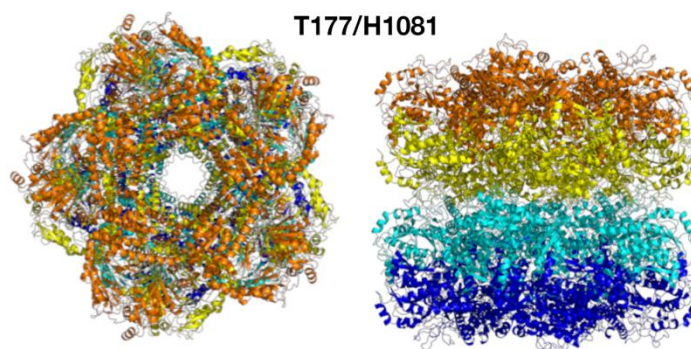
Performance:

Predictions: We participated in 13 prediction targets (all except T168). According to results presented at the CASP14 meeting, our method correctly predicted structures for targets: T177 (Interface 3, **) and T170 (Interfaces: Z:Z and D:D both *). Final models for both targets were selected based on either Hex or KSENIA⁹ scores, which were specifically developed for scoring oligomeric structures.

Scoring: We participated in all 14 scoring targets and our general performance is as follows: 1* hit per Top-1 model, 5*/1** hits per Top-5 models, and 5*/1** hits per Top-10 models. To score the models, we combined our 4 QA methods. All of them were initially designed for scoring monomeric models only. Therefore, the interface scores in the assemblies can be incorrect and noisy.

Difficulties encountered:

For several targets, we did not follow our standard protocol because of their specificity. For the T165/H1036 target with the stoichiometry (ABC)₃, firstly we ran our trimeric docking algorithm DockTrina (a protein docking method for modeling the 3D structures of nonsymmetrical triangular trimers)¹³ for the trimer ABC. Initial models for subunit A were taken from the CASP's T1036s1 stage-2 server predictions. Subunits B and C were modeled with iTASSER⁶ v.5.1. Then, we applied SAM using the C3 symmetry on top of the obtained DockTrina predictions to generate the required stoichiometry.



** Capri prediction quality for a stacking interface

The T190/H1099 target was modeled using an exhaustive scan of all 150 CASP14 stage-2 server submissions using SAM for the 2-fold and 3-fold symmetry axes in the asymmetric subunit. Then, the predictions were supplemented with 60 icosahedral symmetry operators between the asymmetric subunits, and a local optimization with the KSENIA potential⁹, sidechain repacking, and an interactive in-house docking application applied¹². We ranked the predictions according to the KSENIA scores.

We modeled the T170/H1060 and T177/H1081 targets starting from the general protocol for the homo-oligomers. To generate a monomeric subunit of H1081, we used Swiss-Model⁷ with 2VYC as a template. We used experimental structures for subunits in rings A and D. We applied D5 symmetry to H1081, C3 symmetry to the A and B subunits of H1060, C12 symmetry to the C subunit of T170/H1060, and C6 symmetry to the D subunit of T170/H1060. We stacked the two D5 dimers of T177/H1081 and the rings A and B of T170/H1060 using SAM extended to helical symmetries. The other rings in T170/H1060 were stacked along the symmetry axis using the Hex docking engine with only 2 degrees of freedom active, the translation between the subunits, and the twist angle between them. We ranked the T170/H1060 models based on the Hex docking scores. The T177/H1081 models were additionally optimized and ranked using KSENIA⁹.

Availability

More information about our methods can be found at <https://team.inria.fr/nano-d/software>.

References

- 1.Igashov,I., Olechnovic,K., Kadukova,M., Venclovas,C., and Grudin,S. (2021) *Bioinformatics*, btab118, In Press.
- 2.Pagès,G., Charmettant,B., & Grudin,S. (2019). *Bioinformatics*, 35(18), 3313-3319.
- 3.Karasikov,M., Pagès,G., & Grudin,S. (2019). *Bioinformatics*, 35(16):2801-2808.
- 4.Ritchie,D.W., & Grudin,S. (2016). *J. Appl. Cryst.* 49, 158-167.
- 5.Ritchie,D.W., & Kemp,G.J. (2000). *Proteins*, 39: 178-194.
- 6.Yang,J., Yan,R., Roy,A., Xu,D., Poisson,J., Zhang,Y. (2015). *Nat. Methods*, 12: 7-8.
- 7.Waterhouse,A., Bertoni,M., Bienert,S., Studer,G., Tauriello,G., Gumienny,R., Heer,FT, de Beer,TAP, Rempfer,C., Bordoli,L., Lepore,R., Schwede,T. (2018). *Nucleic Acids Res.* 46 (W1), W296-W303.
- 8.Igashov, I., Pavlichenko, N., & Grudin, S. (2020). *arXiv preprint arXiv:2011.07980*.
- 9.Popov,P., & Grudin,S. (2015). *J. Chem. Inf. Model.* 55, 10, 2242–2255.
- 10.Pagès,G., Kinzina,E., & Grudin,S. (2018). *J. Struct. Biol.*, 203(2), 142-148.
- 11.Pagès,G., & Grudin,S. (2018). *J. Struct. Biol.*, 203(3), 185-194.
- 12.Grudin,S., & Redon,S. (2010). *J. Comput. Chem.*, 31(9), 1799-1814.
- 13.Popov P, Ritchie DW, Grudin S. (2014). *Proteins*. 82(1), 34-44.

XI. Integrating residue-residue contact prediction and hybrid scoring function into hybrid docking in CASP14-CAPRI

Yumeng Yan¹, Hao Li¹, Peicong Lin¹, and Sheng-You Huang^{1*}

¹ – School of Physics, Huazhong University of Science and Technology, Wuhan, China, 430074

*Email: huangsy@hust.edu.cn

Methods

During the CASP14-CAPRI experiment, we integrated template-based docking and *ab-initio* docking into a hybrid docking protocol, which is similar to that used in our HDOCK webserver [1, 2] and that used by our group in CASP 13-CAPRI [3], to predict the complex structures for the given targets. Specially, for a given protein sequence, the HHblits [4] program was first used to search against the PDB database for the monomer templates. Then the searched templates were filtered by 20% cutoff of sequence identity and 80% cutoff of sequence coverage. If no templates were found through the filter, the cutoff of the sequence identity was relaxed to 15%-20%. For the hetero-oligomer target, the complex template was selected from the common PDB templates of receptor and ligand according to the sequence identity, sequence coverage and the resolution of the template structure. For the homo-oligomer target, the homo-oligomeric template with the same stoichiometry given by CAPRI organizers was selected. If a complex template was found, MODELLER[5] was subsequently adopted to construct the monomer structure(s) of the target using the corresponding component(s) as monomer template(s). Otherwise, the best monomer template(s) was/were used for homology modeling. Then template-based docking was performed by superimposing the modeled monomer structure(s) onto the complex template if found. The *ab-initio* docking was performed using our HDOCK-lite [6] for hetero-complex target or our HSYMDOCK-lite [7] for homo-complex. A new hybrid scoring function was used to rank the sampled binding modes of *ab-initio* docking. The hybrid scoring function is a linear combination of our distance-based iterative scoring function ITScorePP [8] and the contact-based scoring function IFACE previously used in ZDOCK [9]. At last, the template-based model of the complex and the ranked *ab-initio* docking models were combined together and clustered with an L_{rmsd} cutoff of 5 Å. The selected models were further refined and then submitted. For homo-oligomer targets, a deep learning model, named as DeepHomo [10], was used to predict the inter-protein residue-residue contacts, by integrating evolutionary coupling, sequence conservation, distance map, docking pattern, and physic-chemical information of monomers. Then the top prediction was used to filter the *ab-initio* docking models in the last step. The overall workflow of our hybrid docking protocol is shown in **Figure 1**.

Performance

The hybrid scoring function has been tested in protein-protein docking benchmark 4.0 and outperformed the previous scoring function ITScorePP. When separately tested on the benchmark, IFACE and ITScorePP have shown a complementary effect in terms of characterizing protein-protein interactions. Therefore, the combination of two scoring functions improved the top 1 success rate from 7.4% to 12.5% in unbound docking. DeepHomo model has been tested on a test set of 300 targets with experimental monomer structures and 28 CASP-CAPRI targets with predicted monomer structures. It has shown a much better performance than direct-coupling analysis (DCA) and machine learning (ML)-based approaches, and obtained the precisions of top 1 prediction more than 60%. Integrating the predicted contacts into *ab-initio* docking also significantly improved the top 5 success rate from 42.9% to 64.3% when tested on the 28 realistic CASP-CAPRI targets.

Difficulties

The most difficult thing we encountered in this round was how to integrate the residue-residue contact predictions into the docking protocol efficiently. As now, we only use the top prediction to filter the sampled binding modes. Another challenge was the refinement of the complex models especially the template-based complex model.

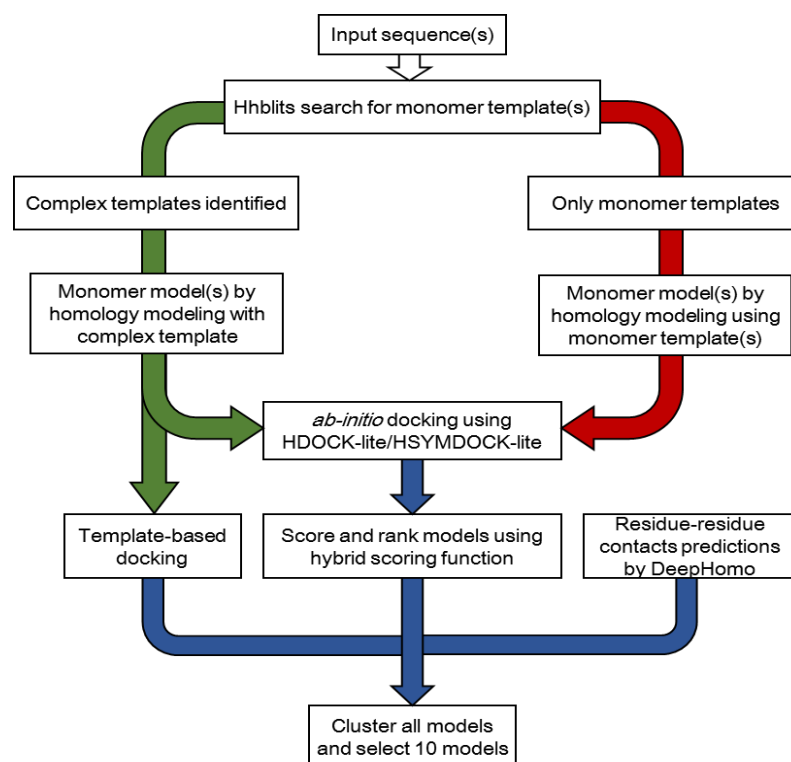


Figure 1: Workflow of our hybrid docking

1. Yan, Y., et al., *The HDOCK server for integrated protein-protein docking*. Nat Protoc, 2020. **15**(5): p. 1829-1852.
2. Yan, Y., et al., *HDOCK: a web server for protein-protein and protein-DNA/RNA docking based on a hybrid strategy*. Nucleic Acids Res, 2017. **45**(W1): p. W365-W373.
3. Yan, Y., et al., *Challenges and opportunities of automated protein-protein docking: HDOCK server vs human predictions in CAPRI Rounds 38-46*. 2020.
4. Remmert, M., et al., *HHblits: lightning-fast iterative protein sequence searching by HMM-HMM alignment*. Nature methods, 2012. **9**(2): p. 173-175.
5. Webb, B. and A. Sali, *Comparative protein structure modeling using MODELLER*. Current protocols in bioinformatics, 2016. **54**(1): p. 5.6. 1-5.6. 37.
6. Yan, Y. and S.Y. Huang, *Pushing the accuracy limit of shape complementarity for protein-protein docking*. BMC Bioinformatics, 2019. **20**(Suppl 25): p. 696.
7. Yan, Y., H. Tao, and S.-Y. Huang, *HSYMDOCK: a docking web server for predicting the structure of protein homo-oligomers with Cn or Dn symmetry*. Nucleic acids research, 2018. **46**(W1): p. W423-W431.
8. Huang, S.Y. and X. Zou, *An iterative knowledge -based scoring function for protein-protein recognition*. Proteins: Structure, Function, and Bioinformatics, 2008. **72**(2): p. 557-579.
9. Chen, R., L. Li, and Z. Weng, *ZDOCK: An initial-stage protein-docking algorithm*. Proteins: Structure, Function, and Bioinformatics, 2003. **52**(1): p. 80-87.
10. Yan, Y. and S.-Y. Huang, *Accurate prediction of inter-protein residue-residue contacts for homo-oligomeric protein complexes*. Briefings in Bioinformatics, 2021.

XII. Kihara human team and LZerD server performance in CAPRI 50 / CASP 14

Charles Christoffer¹, Genki Terashi², Jacob Verburgt², Daipayan Sarkar², Tunde Aderinwale¹, Xiao Wang¹, & Daisuke Kihara^{1,2,*}

¹*Department of Computer Science, Purdue University, USA*

²*Department of Biological Sciences, Purdue University, USA*

We report the protein docking prediction pipeline of our group and the results for CAPRI50/CASP14. The pipeline integrates programs developed in our group as well as other existing scoring functions and modeling tools. HHpred¹ and PSI-BLAST² with default settings were used to search for template structures for the complex structure. If one or more templates of the complex are found, models were generated using MODELLER³. When subunit structures were otherwise unavailable, structures generated by our CASP14 free modeling (de novo) pipeline were used⁴.

If templates of the full complex were not found in the PDB, we generated ab initio docking models using the LZerD protein-protein docking algorithm developed in our group⁵. In cases of complexes with more than two subunits, a restricted and modified version of the multiple-chain docking protocol Multi-LZerD⁶, developed in our group, was used on top of LZerD. Partial complex templates and symmetry information were integrated. In the case of human group prediction, we surveyed the literature to find information to guide the modeling, such as protein-protein interface information. We also integrated available SAXS data, but the applicable target was canceled. In addition to any literature information, generated docking decoys were selected by a combination of scoring functions, including DFIRE⁷, GOAP⁸, and ITScorePro⁹. These scores were combined by the simple rank aggregation scheme of adding their numerical rank values, called ranksum¹⁰. The top ten decoys were relaxed by a short molecular dynamics simulation before submission to remove atom clashes and improve side-chain conformations.

Performance Summary

In CAPRI50/CASP14, our groups ranked near the top of the preliminary assessment released in December 2020. For prediction, our human and server groups produced models of at least acceptable quality for 7 and 6 targets respectively, as well as models of at least medium quality for 3 and 2. Broken down by modeling category, our human and server groups achieved at least acceptable quality for 9 and 3 target-interfaces respectively for targets where ab initio docking was used. Of the 3 targets where de novo subunit structure prediction was relied on exclusively, we were able to achieve acceptable complex models for 2 of them. Templates used are listed in Table 1.

Success

Our docking pipeline achieved acceptable model quality for T179, a bacterial prototoxin, although no templates for either the complex or for the subunit were found. Our T179 models were generated by modeling the subunit de novo and then docking de novo models using LZerD in C2 symmetry mode (see Figure 1). LZerD was one of only two servers to acceptably model this target.

Failure/Challenges

T170 was a particularly challenging target. This phage tail complex with A6B3C12D6 stoichiometry would have likely been impossible as a completely ab initio target. Of the 9 interfaces in this target, we were able to acceptably model 5. Particularly, 2 of the interfaces that we modeled acceptably were classified as difficult by the organizers; only one other group was able to model 2 difficult interfaces, and no groups were able to model all the difficult interfaces. These difficult interfaces were within the 12-chain cyclic ring, between that cyclic ring and the concentric 3-chain cyclic ring, and within that 3-chain ring. We were the only group to successfully model one of the specific interfaces between the two rings. However, the other such interface was missed. Furthermore, we missed 3 of the 4 easy interfaces among the two stacked 3-chain cyclic identical-sequence rings, despite the fact that most groups which succeeded on any interface of this target were able to model at least 2 of those interfaces.

Figure 1. T179 acceptable LZerD server model.

LZerD server model #4 is shown in green and cyan. At 78% sequence recovery, this model is of acceptable quality with an f_{na} of 0.30 and an L-RMSD of 9.1 Å. At time of writing, the native structure was not publicly available and so is omitted here.

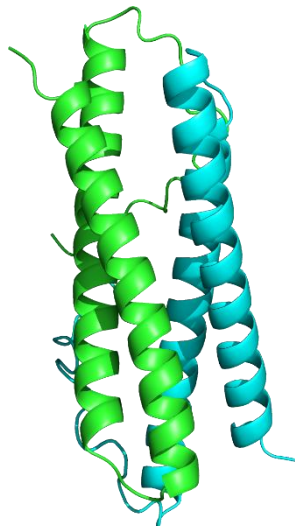


Table 1. Templates used for all evaluated CAPRI 50 submissions.

Targets where no template was used for subunit modeling as well as for the assembly are marked “n/a”. A template being listed does not indicate that de novo models were not also used for that target.

Target	List of templates
T164	4RSJ
T165	2GUM, 4PFE, 5JYM, 5C6T, 3FVC, 3NWA, 5V2S, 6ESC
T166	4BWF, 5NKZ
T168	3DC7, 6F7D
T169	n/a
T170	3UH8, 5NGJ, 6F2M, 5IV5
T174	1S2E
T176	3V0R
T177	2VYC
T178	n/a
T179	n/a

T180

3J2V

Funding

This work was partly supported by the National Institutes of Health (R01GM123055). CC was supported by NIGMS-funded predoctoral fellowship to CC (T32 GM132024).

References

1. Zimmermann L, Stephens A, Nam SZ, et al. A Completely Reimplemented MPI Bioinformatics Toolkit with a New HHpred Server at its Core. *J Mol Biol.* 2018;430(15):2237-2243.
2. Altschul SF, Madden TL, Schaffer AA, et al. Gapped BLAST and PSI-BLAST: a new generation of protein database search programs. *Nucleic Acids Res.* 1997;25(17):3389-3402.
3. Sali A, Blundell TL. Comparative protein modelling by satisfaction of spatial restraints. *J Mol Biol.* 1993;234(3):779-815.
4. Jain A, Terashi G, Kagaya Y, Maddhuri Venkata Subramaniya SR, Christoffer C, Kihara D. Analyzing Effect of Quadruple Multiple Sequence Alignments on Deep Learning based Protein Inter-Residue Distance Prediction. *In submission.* 2021.
5. Esquivel-Rodriguez J, Filos-Gonzalez V, Li B, Kihara D. Pairwise and multimeric protein-protein docking using the LZerD program suite. *Methods Mol Biol.* 2014;1137:209-234.
6. Esquivel-Rodriguez J, Yang YD, Kihara D. Multi-LZerD: multiple protein docking for asymmetric complexes. *Proteins.* 2012;80(7):1818-1833.
7. Zhou H, Zhou Y. Distance-scaled, finite ideal-gas reference state improves structure-derived potentials of mean force for structure selection and stability prediction. *Protein Sci.* 2002;11(11):2714-2726.
8. Zhou H, Skolnick J. GOAP: a generalized orientation-dependent, all-atom statistical potential for protein structure prediction. *Biophys J.* 2011;101(8):2043-2052.
9. Huang SY, Zou X. Statistical mechanics-based method to extract atomic distance-dependent potentials from protein structures. *Proteins.* 2011;79(9):2648-2661.
10. Christoffer C, Terashi G, Shin WH, et al. Performance and enhancement of the LZerD protein assembly pipeline in CAPRI 38-46. *Proteins.* 2019.

XIII. Template-based Structure Prediction and Inter-residue Distances and Orientations Prediction-based Structure Prediction

Tsukasa Nakamura, and Yuya Hanazono^{1,2}

¹*Tsukasa Nakamura; Graduate School of Information Sciences, Tohoku University, Sendai, Miyagi, 980-8579, Japan;*

²*Yuya Hanazono; Institute for Quantum Life Science, National Institutes for Quantum and Radiological Science and Technology, Tokai, Ibaraki, 319-1106, Japan*

In CAPRI 50 (CASP 14), we used a multiple sequence alignment (MSA) generated by our method¹ as a seed input for HHblits² to perform profile-profile sequence search, and we also used the template profile database created in a similar method. To construct 3D-models, we used template-based structure prediction by MODELLER³, interresidue distances and orientations prediction-based structure prediction by trRosetta⁴, and combined them in some targets. In addition, we predicted quaternary structures that replicate experimental evidence based on a literature search.

Methods

To execute a sequence search of a target, we used SSearch⁵ with MIQS⁶ against the latest NCBI nr database. Then we made an MSA by using MPI-parallelized MAFFT^{7,8} with

homologous sequences. With the MSA as input, we used HHblits to execute an iterative profile–profile sequence search against the UniClust30⁹ and BFD¹⁰ databases.

To execute a template search and acquire profile–profile alignment between target and templates, we used HHsearch² against the latest PDB70 and an in-house profile database that was made by three iterations of HHblits with MSAs as input. These MSAs were made with PDB98 against NCBI nr in a similar manner for target sequences. However, we made the MSAs partly by stacking pairwise sequence alignments by SSearch instead of using MPI-parallelized MAFFT.

In our 3D-model construction step, we used MODELLER with the result of the profile–profile alignment against PDBs and trRosetta with the result of the sequence search. We intervened in the processes of trRosetta by partly substituting the input with the distances and orientations of 3D-models made by MODELLER in some targets that had good templates and made 3D-models well.

In our model selection step, we used VoroMQA¹¹ mainly, dDFire¹², ProQ4¹³, and the rate of fit with the servers' distance predictions.

For multimeric targets, the stoichiometry of the template protein was considered to select a model. Also, experimental evidence (e.g., the number of disulfide bonds by mass spectrometry and interacting regions by pull-down assay) based on a literature search was heavily considered and we tried to replicate the evidence in 3D-models by adding restraints manually. If we needed to perform free-docking, we used Haddock¹⁴ and ZDOCK¹⁵. If we considered that the target must be coiled-coil but it was hard to construct a model, we used ISAMBARD¹⁶.

Performance

In CAPRI 50, our group was able to submit models for 9 out of the 12 targets (if including cancelled and no structure targets, 15 out of the 18 targets). In the preliminary assessment, our models achieved medium quality for 2 targets (T166, T170K:L(Z:Z)) and acceptable quality for 3 targets (T164, T170A:B(A:A), T177). Regarding T166, we superimposed a good server model for PEX4 and a model which we produced for PEX22 to the interface structure of 2y9m. Regarding T170K:L, we superimposed a good server model to 6v8i. Regarding T170A:B, we used Fit in Map of UCSF Chimera with EMD-3691 and 5ngj.

Failure

In the case of T168, although we produced the multimeric structure of domain 1 (1-539) based on 6f7k, we misplaced the other domains and it caused too many clashes (presumably more than the disqualification threshold).

Acknowledgments

This work was supported by the Japan Society for the Promotion of Science KAKENHI (Grant Number JP19J00950 to T.N.). Computations were partially performed on the ToMMo supercomputer system in Tohoku University, the Reedbush System in the Information Technology Center, the University of Tokyo, and the NIG supercomputer at ROIS National Institute of Genetics.

References

1. Nakamura,T., Oda,T., Fukasawa,Y., and Tomii,K. (2018) Template-based quaternary structure prediction of proteins using enhanced profile–profile alignments. *Proteins Struct. Funct. Bioinforma.*, **86**, 274–282.
2. Steinegger,M., Meier,M., Mirdita,M., Vöhringer,H., Haunsberger,S.J., and Söding,J. (2019) HH-suite3 for fast remote homology detection and deep protein annotation. *BMC Bioinformatics*, **20**.

3. Webb,B. and Sali,A. (2016) Comparative protein structure modeling using MODELLER. *Curr. Protoc. Bioinforma.*, **2016**, 5.6.1-5.6.37.
4. Yang,J., Anishchenko,I., Park,H., Peng,Z., Ovchinnikov,S., and Baker,D. (2020) Improved protein structure prediction using predicted interresidue orientations. *Proc. Natl. Acad. Sci. U. S. A.*, **117**, 1496–1503.
5. Pearson,W. (2003) Finding Protein and Nucleotide Similarities with FASTA . *Curr. Protoc. Bioinforma.*, **4**.
6. Yamada,K. and Tomii,K. (2014) Revisiting amino acid substitution matrices for identifying distantly related proteins. *Bioinformatics*, **30**, 317–325.
7. Nakamura,T., Yamada,K.D., Tomii,K., and Katoh,K. (2018) Parallelization of MAFFT for large-scale multiple sequence alignments. *Bioinformatics*, **34**, 2490–2492.
8. Katoh,K. and Standley,D.M. (2013) MAFFT multiple sequence alignment software version 7: Improvements in performance and usability. *Mol. Biol. Evol.*, **30**, 772–780.
9. Mirdita,M., Von Den Driesch,L., Galiez,C., Martin,M.J., Soding,J., and Steinegger,M. (2017) Uniclust databases of clustered and deeply annotated protein sequences and alignments. *Nucleic Acids Res.*, **45**, D170–D176.
10. Steinegger,M., Mirdita,M., and Soding,J. (2019) Protein-level assembly increases protein sequence recovery from metagenomic samples manifold. *Nat. Methods*, **16**, 603–606.
11. Olechnovič,K. and Venclovas,Č. (2017) VoroMQA: Assessment of protein structure quality using interatomic contact areas. *Proteins Struct. Funct. Bioinforma.*, **85**, 1131–1145.
12. Yang, Y. and Zhou, Y. (2008) Specific interactions for ab initio folding of protein terminal regions with secondary structures. *Proteins-Structure Funct. Bioinforma.*, **72**, 793–803.
13. Hurtado,D.M., Uziela,K., and Elofsson,A. (2018) Deep transfer learning in the assessment of the quality of protein models. *arXiv*.
14. Dominguez,C., Boelens,R., and Bonvin,A.M.J.J. (2003) HADDOCK: A protein-protein docking approach based on biochemical or biophysical information. *J. Am. Chem. Soc.*, **125**, 1731–1737.
15. Chen,R., Li,L., and Weng,Z. (2003) ZDOCK: An initial-stage protein-docking algorithm. *Proteins Struct. Funct. Genet.*, **52**, 80–87.
16. Wood,C.W. *et al.* (2017) ISAMBARD: An open-source computational environment for biomolecular analysis, modelling and design. *Bioinformatics*, **33**, 3043–3050.

XIV. CAPRI Round 50 Extended Abstract, Pierce Team

Ragul Gowthaman^{1,2}, Johnathan D. Guest^{1,2}, Rui Yin^{1,2}, Ghazaleh Taherzadeh^{1,2}, and Brian G. Pierce^{1,2}

¹*University of Maryland Institute for Bioscience and Biotechnology Research, Rockville, MD 20850, USA*

²*Department of Cell Biology and Molecular Genetics, University of Maryland, College Park, MD 20742, USA*

Our team submitted models for 17 out of 18 targets, and 11 of our submitted targets were evaluated out of the 12 evaluated targets. Our basic modeling strategy for this CAPRI round entailed these main steps: 1) Select monomer structure(s) from the CASP server model sets, 2) Utilize one or more of the following docking protocols: RosettaDock¹, ZDOCK 3.0.2², SymDock³ and M-ZDOCK⁴ (the latter two for C_n symmetric docking), 3) Refinement and model selection, including one or more of the following protocols: clustering using FCC⁵, model refinement using Rosetta FastRelax⁶ or local RosettaDock, and re-scoring with ZRANK2⁷ and Rosetta REF15⁸ scoring functions. For ZDOCK and M-ZDOCK docking input, certain residues or regions were blocked to avoid their participation in modeled interfaces, when information from known structures or the literature was identified by our team.

Table 1 summarizes the methods and results for all evaluated targets from our team. Our multi-stage strategy, which utilized a range of available tools, achieved Acceptable or

better models for 7 targets, including Medium or higher quality models for four targets (T166, T168, T177, T180). Also, for two homodimeric targets classified as Difficult, we generated Acceptable quality models (T178, T179). Among 47 CASP teams that participated in CASP-CAPRI targets, our team was ranked 7th based on average z-score (> 0.0). While for most targets we used major docking and refinement tools, for the large ring-shaped assemblies of T170 and T177 we performed template-based homomultimer modeling with SWISS-MODEL⁹, in conjunction with PyMOL (Schrodinger, Inc.) to position the rings in the respective assemblies. Lack of successful predictions for four Difficult targets (T169, T170, T174, T176) highlights the need for improved docking protocols in scenarios with conformational changes in unbound or modeled input structures.

Table 1. Prediction methods and results for evaluated targets.

Target	Assembly	Quality ¹	Server Model(s) ²	Methods ³	Difficulty
T164	Homodimer	Acceptable	Zhang-Server BAKER-ROSETTASERVER MULTICOM-DEEP RaptorX	SymDock, M-ZDOCK, FastRelax	Easy
T166	Heterodimer	Medium	Zhang-Server ZhangS	RosettaDock ZDOCK FastRelax	Easy
T168	Homotrimer	Medium	ZhangS MultiAI	FastRelax	Easy
T169	Homodimer	Incorrect	RaptorX, Zhang_Ab_Initio	M-ZDOCK, FastRelax, ZRANK2, FCC	Difficult
T170.1-9	Homultimer/Heteromultimer rings	Incorrect (Interface 1-9)	SWISS-MODEL Templates: 5NGJ	MZDOCK, PyMOL	Difficult
T174	Homotrimer	Incorrect	Zhang-Server, Zhang-CEthreader, Quark	Assembly templates: 5HX2, 1QEX FastRelax, ZRANK2	Difficult
T176	Homodimer	Incorrect	BAKER-ROSETTASERVER	M-ZDOCK, SymDock, FastRelax, ZRANK2	Difficult
T177.1 T177.2 T177.3	Two stacked decamers	High (Interface 1) High (Interface 2) Medium (Interface 3)	SWISS-MODEL Template: 2VYC	PyMOL	Easy
T178	Homodimer	Acceptable	Zhang-Server MUFOLD2	M-ZDOCK, SymDock	Difficult
T179	Homodimer	Acceptable	BAKER-ROSETTASERVER	M-ZDOCK, FastRelax, SymDock, FloppyTail, ZRANK2	Difficult
T180.1 T180.2	Capsid	Incorrect (Interface 1) Medium (Interface 2)	BAKER-ROSETTASERVER Zhang-Server Yang-Server MULTICOM-DIST	Assembly templates: 6HTX, 1QGT SymDock, FastRelax, ZRANK2	Easy

¹Best CAPRI model rating in top 5 submitted structures.

²CASP server model used as docking/modeling input. In most cases, the top model from the specified server (“TS1”) was used in modeling.

³Methods used for docking and/or refinement: RosettaDock¹, ZDOCK², SymDock³, M-ZDOCK⁴, FCC⁵, Rosetta FastRelax⁶, ZRANK2⁷, PyMOL (Schrodinger, Inc.), SWISS-MODEL⁹. PDB codes for multimeric structures used to guide or fit assemblies are also noted.

References

1. Gray JJ, Moughon S, Wang C, et al. Protein-protein docking with simultaneous optimization of rigid-body displacement and side-chain conformations. *J Mol Biol.* 2003;331(1):281-299.
2. Pierce BG, Hourai Y, Weng Z. Accelerating protein docking in ZDOCK using an advanced 3D convolution library. *PLoS One.* 2011;6(9):e24657.
3. Andre I, Bradley P, Wang C, Baker D. Prediction of the structure of symmetrical protein assemblies. *Proc Natl Acad Sci U S A.* 2007;104(45):17656-17661.
4. Pierce B, Tong W, Weng Z. M-ZDOCK: a grid-based approach for Cn symmetric multimer docking. *Bioinformatics.* 2005;21(8):1472-1478.
5. Rodrigues JP, Trellet M, Schmitz C, et al. Clustering biomolecular complexes by residue contacts similarity. *Proteins.* 2012;80(7):1810-1817.
6. Khatib F, Cooper S, Tyka MD, et al. Algorithm discovery by protein folding game players. *Proc Natl Acad Sci U S A.* 2011;108(47):18949-18953.
7. Pierce B, Weng Z. A combination of rescoring and refinement significantly improves protein docking performance. *Proteins.* 2008;72(1):270-279.
8. Alford RF, Leaver-Fay A, Jeliakov JR, et al. The Rosetta All-Atom Energy Function for Macromolecular Modeling and Design. *J Chem Theory Comput.* 2017;13(6):3031-3048.
9. Waterhouse A, Bertoni M, Bienert S, et al. SWISS-MODEL: homology modelling of protein structures and complexes. *Nucleic Acids Res.* 2018;46(W1):W296-W303.

XV. Oliva team performance, CASP14-CAPRI, Round 50

Didier Barradas-Bautista¹, Zhen Cao¹, Luigi Cavallo¹ and Romina Oliva^{2*}

¹ King Abdullah University of Science and Technology, Saudi Arabia

² University of Naples “Parthenope”, Italy

*E-mail: romina.oliva@uniparthenope.it

Scoring function/scheme used

We submitted scoring predictions for all the 14 targets assessed in the scoring experiment, using an approach similar to the one we first applied in the CASP13/CAPRI round. In order to assign a tentative easy/difficult classification to each target, as a preliminary step, we used HHPRED [1] to search for possible templates for the modeling of the single proteins and of the assembly. All the targets (with the partial exception of T170 and T177, see below) were scored with our tools CONSRANK (CONsensus RANKing) and Clust-CONSRANK. CONSRANK is a pure consensus method for the ranking of docking decoys [2-3]. It calculates the frequency of inter-molecular contacts in a decoys ensemble and then ranks each decoy based on its ability to match the most frequent contacts. Clust-CONSRANK is a CONSRANK implementation introducing a contact-based clustering of the models as a preliminary step of the scoring process [4]. For the clustering, a threshold on the number of clusters was set as 1/10 of the total number of models per target.

For each target, the \approx 20-30 models with the highest CONSRANK score and the 3-4 top ranked models for the 15 most populated clusters from the Clust-CONSRANK output were further analyzed with CoCoMaps [5], a web tool we developed for the analysis of the

interface in macromolecular complexes. Models showing a large number of clashes were removed from the selection. The weaker was the overall consensus highlighted by CONSRANK, the higher was the number of models we selected from the Clust-CONSRANK output. Ranking of the selected models from the top-1 to the top-10 position was guided by results of the interface analysis, especially in terms of extension of the contacts network and of the interface area.

Models for the hetero 27-mer T170 and the homo 20-mer T177 target were analysed by CONSRANK focusing on single interfaces and also subjected to short *in vacuo* molecular dynamics (MD) simulations, carried out with GROMACS in a microcanonical (NVE) ensemble [6]. The MD simulations were followed by a clustering step to single out representatives of the different clusters. Submitted models for these two targets were partially selected from the CONSRANK results, partially from the MD approach.

Short description of successes and failures

Our performance was especially effective in the top-1 ranking, where we were second, with at least one correct solution for 6 targets, of which 3 of medium quality (see Figure 1), on a par with Takeda-Shitaka, and second after LZERD, which exceeded our performance for having one target with a top-1 high quality model instead of a medium-quality one.

Our performance for the top-5 ranking coincides with that for the top-1 ranking. As for the top-10 ranking, we submitted correct models for 7 targets, for 1 of them of high quality- and for 2 of them of medium-quality. This compares with the 9 targets with at least one correct model, of which 4 of medium quality, of the best performing scorers in this CAPRI Round.

Our successful targets (both in the top-1 and top-5 rankings) correspond to T164, T166, T168, T177, T178 and T179, which include different types of homo- and hetero-assemblies. The targets for which we could not submit any correct solutions (at the top-10 positions), while at least another scorer could, were instead T176 and T180. These targets, a homodimer and a 240-mer assembly, respectively, were particularly difficult ones, for which most of the scorer groups could not identify any correct solution. These are most probably targets whose scoring sets included only very few correct models and remain the critical cases for us.

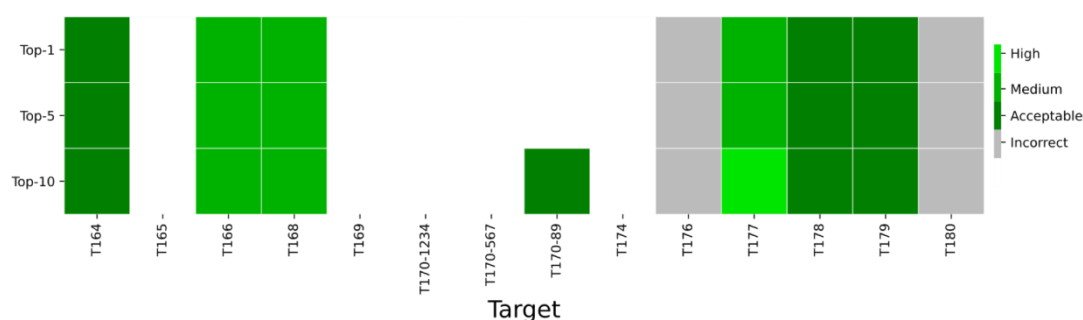


Figure 1. Our performance (Oliva's group) as scorers for the 14 assessed targets of the CASP14/CAPRI50 joint experiment. The presence of high, medium quality, acceptable or incorrect models in each ranking is reported in a green-to-gray color code. Targets for which no acceptable solutions were available are colored white.

References

1. Söding J, Biegert A, Lupas AN. (2005) *Nucleic Acids Res.* **33**:W244-8.
2. Oliva, R, Vangone, A and Cavallo, L (2013) *Proteins* **81**, 1571-1584.

3. Chermak, E, Petta, A, Serra, L, Vangone, A, Scarano, V, Cavallo, L, Oliva, R (2015) *Bioinformatics* **31**, 1481-3.
4. Chermak, E, De Donato, R, Lensink MF, Petta, A, Serra, L, Scarano, V, Cavallo L, Oliva R (2016) *PLoS One* **11**:e0166460.
5. Vangone A, Spinelli R, Scarano V, Cavallo L, Oliva R. (2011) *Bioinformatics* **27**:2915.
6. Van Der Spoel D, Lindahl E, Hess B, Groenhof G, Mark AE, Berendsen HJ. (2005) *J Comput Chem.* **26**:1701.

XVI. Performance of the Shen team in CASP14-CAPRI Round 50

Yuanfei Sun, Shaowen Zhu, and Yang Shen*

*Department of Electrical and Computer Engineering, Texas A&M University,
College Station, TX 77843, USA*

* E-mail: yshen@tamu.edu

Methods

We first adopted monomer structures from CASP14 tar ball (stage 2 webserver predictions, specifically “Zhang-Server”, “BAKER-ROSETTASERVER”, and “RaptorX”) and performed rigid docking using the web server ClusPro. Multimer docking, antibody mode, and attractions were used in ClusPro whenever applicable. Homology models are built if oligomer templates are identified (we used HHpred for monomer sequences).

We then refined oligomer models using our BAL (Bayesian Active Learning) [1] and rescored the refined models using our EGCN (Energy-based Graph Convolutional Networks) [2].

Our innovations include:

1. *Conformational flexibility: basis directions and ranges.* We used encounter complex-based normal mode analysis, incorporating both effects of conformational selection and induced fit, to predict the directions and the ranges of conformational change (first proposed in [3][4] and then upgraded in BAL [1]).
2. *Conformational search with uncertainty awareness.* By directly modeling the posterior distribution of the unknown global optimum (the native structure), we guide conformational search and improve model scoring with uncertainty estimation [1].
3. *Absolute and relative quality estimation.* In BAL [1], we had developed a funnel-like energy function using random forest of MM-PBSA features, which is used for both absolute quality estimation (iRMSD estimation) and relative quality estimation (ranking/scoring of structure models). For this round of CASP/CAPRI, we have adopted the newly-developed EGCN [2] for both absolute and relative quality estimation, which is the first graph neural networks for the purpose. Compared to our earlier shallow models (random forest in [1]), the new deep-learning model [2] directly learns energy values from 3D structures represented as graphs rather than indirectly doing so from structure-based semi-empirical energy calculations. EGCN was used for both re-scoring our models in the docking experiment and re-scoring community submissions in the scoring experiment.

Performances

In the CASP multimeric evaluation on CAPRI targets only, our submissions for 10 targets led to a sum of Z score (≥ 0.0) being 5.94, placing us 14th out of 47 CASP+CAPRI groups. In particular, our CASP ranking on three hard (FM) targets were 8th/34.

In the CAPRI docking evaluation, our submissions for 12 targets (not counting 2 canceled targets and 4 targets without structures determined) led to at least acceptable prediction for 6 of the 12 targets, including medium-accuracy prediction for 1 target. The docking performance (a sum score of 7) placed us tied 15th out of 28 teams, being 1-point shy of the top 10.

Target-based break downs of our docking performances are as follows. First, for 2 easy dimers, we had one acceptable (T164/T1032) and one medium-accuracy (T166/H1045) prediction. Second, for 4 difficult dimers (T169/T1054, T176/T1078, T178/T1083, T179/T1087), we had acceptable prediction for T169 and T179 whereas the community had at least acceptable prediction for 3 of the 4 (the one where we didn't succeed was T178). Third, for 3 homo-trimers (T165/H1036, T168/T1052, and T174/T1070), we had no acceptable prediction and the community had only such for T168; however, T168 turned out to be easy for the community (19 teams had acceptable prediction, including 2 teams with high accuracy and 9 with medium accuracy). Last, for the 3 remaining targets of cryo-EM hetero-oligomer assemblies including T177/H1081 (the decarboxylase), T180/T1099 (viral capsid), and T170/H1060 (T5 phage tail distal complex), we had at least acceptable prediction for T180 and T170, but we missed T177 which turned out to be easy for the community (16 teams had at least acceptable predictions including 8 teams with medium accuracy and 1 with high accuracy). Taken together, we did well for difficult dimers and the 240-mer T170. In particular, we had at least acceptable prediction for 6 of the 9 interfaces of T170, including 2 interfaces with medium-accuracy prediction, which was the community best. Our models for the difficult T170 interfaces of C3/C5 and min unit also had the highest TM scores among all CASP-assessed submissions. However, our performance was poor for the easy cases of T168 and T177, for which the reasons remain to be validated and may include interfacial clashes in the models.

In the CAPRI scoring evaluation, our submissions for 12 targets (14 interfaces) had identified (among top-5 models) at least acceptable prediction for 7 targets/interfaces, including medium-accuracy prediction for 3 of the 7. The scoring performance placed us tied 7th out of 19 teams. We note that our scoring results included medium-accuracy top-5 models for both T168 and T177.

Challenge

Regardless of the performances, the cryo-EM hetero-assemblies present a major challenge (and potential opportunity) to our pipeline that has mainly been developed for dimers.

Acknowledgement

The study was in part supported by NIH/NIGMS (R35GM124952 to YS) and NSF (CCF-1943008).

References

- [1] Y. Cao and Y. Shen. Bayesian active learning for optimization and uncertainty quantification in protein docking. *Journal of Chemical Theory and Computation* (2020), 16(8), p. 5334-5347.
- [2] Y. Cao and Y. Shen. Energy-based graph convolutional networks for scoring protein docking models. *Proteins* (2020), 88(8), p. 1091-1099.
- [3] T. Oliwa and Y. Shen. cNMA: a framework of encounter complex-based normal mode analysis to model conformational changes in protein interactions (2015). *Bioinformatics* 31(12), p. i151-i160.
- [4] H. Chen, Y. Sun, Y. Shen. Predicting protein conformational changes for unbound and homology docking: learning from intrinsic and induced flexibility (2017). *Proteins* 85(3), p.544-556.

XVII. Predicting protein complex structures using GALAXY in CAPRI round 50

Taeyong Park, Hyeonuk Woo, Jinsol Yang, Sohee Kwon, Jonghun Won, and **Chaok Seok**
Department of Chemistry, Seoul National University, Seoul 08826, Republic of Korea chaok@snu.ac.kr

We participated in CAPRI round 50 as a server group GalaxyPPDock and a human group Seok. GalaxyPPDock submitted server predictions generated by GALAXY programs with minimal human intervention. Human intervention was made only when the stoichiometry of the target did not correspond to A_n or A_1B_1 or when additional information was provided. Human predictions submitted by Seok were also generated by GALAXY, but human intuitions were utilized in selecting monomer models, using information obtained from the literature search, scoring complex models, etc.

Methods

The newly developed GalaxyHomomer2 and GalaxyHeteromer were used to predict the structures of homo-oligomers and hetero-oligomers, respectively, from sequences. These oligomer structure prediction pipelines were run following the monomer modeling pipeline of CASP14 Seok-server. Monomer models, selected among those predicted by template-based modeling GalaxyTBM and by an in-house distance-based modeling method that employs distance prediction from sequence coevolution, were further subject to quaternary structure prediction.

GalaxyHomomer2 performed homo-oligomer structure prediction by template-based and *ab initio* docking depending on template availability, just like GalaxyHomomer. In GalaxyHomomer2, the two template-based modeling methods, sequence-based template detection followed by restraint-based modeling-building and structure-based template detection followed by superimposition-based model building, were re-balanced, considering improved monomer structure prediction owing to improved distance prediction.

GalaxyHeteromer performed automatic hetero-dimer structure prediction also by template-based and *ab initio* docking depending on the availability of hetero-dimer templates. Templates to be used for hetero-dimer modeling were selected from HHsearch high-rankers including monomers and homo-oligomers as well as from a hetero-dimer structure database based on structure similarity between the monomer models and the templates. The hetero-dimer structure database consisted of non-redundant hetero-dimer structures prepared by compiling all hetero-dimers with atomic contacts in PDB and sequence- and structure-based clustering. Hetero-dimer models generated by superimposing the monomer models on the templates were ranked by monomer structure similarity, with additional consideration of the number of clashes, the number of contacting residue pairs, and interface area. If template-based modeling produces less than five models, *ab initio* asymmetric docking method GalaxyTongDock_A was used to generate more models to get a total of five models.

Results and Discussion

We confirmed that there remains a large gap between performances of human and server predictions. In most cases, manual prediction showed higher performance than server prediction, as shown in Figure 1. In the case of T174, incorrect complex structure prediction originated from incorrect monomer structure prediction by the server. However, human prediction started with manual domain splitting of the monomer into four domains, and the trimer structure of each domain was predicted first before full domain docking. The human predictions resulted in a trimer interface of the 2nd domain ($F_{nat}=0.667$) and the 4th domain ($F_{nat}=0.417$) with acceptable quality. In the case of T180, incorporation of key interactions

extracted from mutagenesis studies of capsid protein assembly resulted in an acceptable model, which turned out to be the only acceptable model submitted by all.

As a post-analysis, monomer structures of AlphaFold2 (AF2) were subject to *ab initio* docking with TongDock for eight targets of stoichiometry A_n or A_1B_1 to assess the effect of improved monomer structure quality. In one case (T179), docking of the AF2 monomer model resulted in a medium quality model ($F_{nat}=0.81$) compared to an acceptable quality model ($F_{nat}=0.18$) obtained previously. In the remaining seven cases, AF2 monomer structures had incorrect interface structures, and resulted in incorrect complex structure prediction by docking. In six of the seven cases, superposition of AF2 monomers to the crystal complex structures caused severe steric clashes. So, the current AF2 monomer models do not seem to be enough to be accurately docked by rigid-body docking.

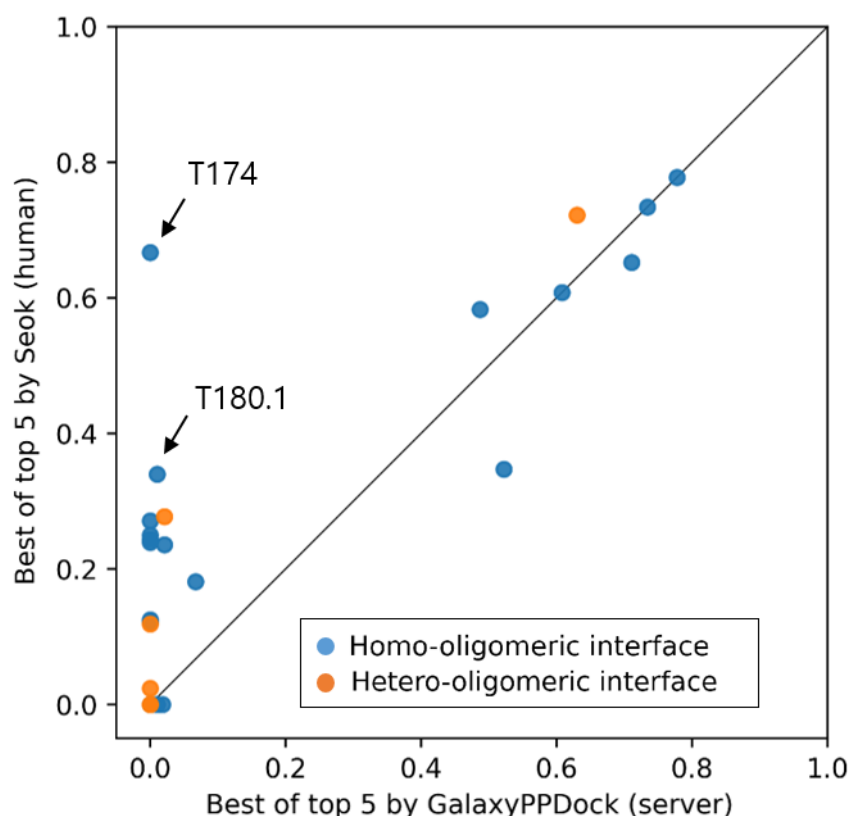


Figure 1. Performance comparison of the server and human predictions in terms of the fraction of native contacts (F_{nat}) for the best of top 5 models. Targets mentioned in the text, T174 and T180.1 (interface 1), are marked with their target numbers.

XVIII. Performance of Takeda-Shitaka Team in CASP14-CAPRI Round 50

Yasuomi Kiyota, Shinpei Kobayashi, Yoshiki Harada and Mayuko Takeda-Shitaka

School of Pharmacy, Kitasato University, Tokyo, Japan

Introduction

We participated in the assembly category of CASP14-CAPRI50. We predicted both homo- and hetero-oligomeric protein structures according to the oligomeric state in the CASP14-CAPRI50 target list. Our modeling procedure was based on template-based docking method.

Methods (Human Predictor)

Monomer model selection

We basically used CASP14 server models (Stage 2) as monomer models. We selected high quality monomer models using combined score of ProQ3¹, ProQ3D² and VoroMQA³. The score was adjusted to pick up high quality models. When we could not obtain high quality server models, we constructed the monomer models by MODELLER⁴ based on alignments from HHalign⁵.

Oligomeric template search

To find reliable oligomeric templates, we carried out two-step template search. Firstly, the oligomeric templates were searched by HHblits⁵ against PDB70 database. Secondly, to search oligomeric templates more widely, we ran PSI-BLAST⁶ on PDBaa using HHblits hits as inputs. According to the results of two-step template search and information of biological unit, oligomeric templates were selected.

Oligomeric model construction

To construct oligomeric models, we performed template-based docking. We superposed the monomer models onto the oligomeric templates using TM-align⁷ or CAB-align⁸. When we could not obtain the oligomeric templates, we used DOCKGROUND⁹ database as templates. For some targets, we used SymDock2¹⁰ to construct the oligomeric models.

Quality assessment and refinement of oligomeric models

The quality of oligomeric models were assessed by combined score of VoroMQA and SOAP-PP¹¹. The selected 5 models were refined using MODELLER to remove steric clashes.

Methods (Scorer)

When oligomeric templates were available, oligomeric models were superposed onto oligomeric templates using MM-align¹². Models with insufficient TMscore or many clashes in the interface were removed before scoring. The same scoring method for human prediction was used for scoring models. Based on the results, 10 models were selected.

Successes and Failures

For T166, our model was assessed as high (***) by the CAPRI measure. We could find a good oligomeric template (PDB ID: 2Y9M) and select good monomer models from the CASP14 server models (step2) for both chains using our method described above.

T170 was a challenging target because it was 27-mer and had many interfaces. This hetero-complex target had ring A (A3), ring B (A3), ring C (B3/C12) and ring D (D6). We prepared ring-shaped templates for each ring (5NGJ for ring A and B, 6F2M for ring C, and 4JMQ for ring D). After constructing these rings, we assembled whole structure based on two templates (6V8I and 4V96). It was difficult to remove steric clashes. As a result, two out of nine interfaces of our model were assessed as acceptable (*) by the CAPRI measure.

References

1. Uziela K, Shu N, Wallner B, Elofsson A. ProQ3: Improved model quality assessments using Rosetta energy terms. *Scientific reports*. 2016;6:33509.
2. Uziela K, Menéndez Hurtado D, Shu N, Wallner B, Elofsson A. ProQ3D: Improved model quality assessments using Deep Learning. *Bioinformatics*. 2017;33(10):1578-1580.
3. Olechnovič K, Venclovas Č. VoroMQA: Assessment of protein structure quality using interatomic contact areas. *Proteins*. 2017;85(6):1131-1145.
4. Sali A, Blundell TL. Comparative protein modelling by satisfaction of spatial restraints. *J. Mol. Biol.* 1993;234(3):779-815.
5. Steinegger M, Meier M, Mirdita M, Vöhringer H, Haunsberger SJ, Söding J. HH-suite3 for fast remote homology detection and deep protein annotation. *Bioinformatics*. 2019;20(1):473.
6. Altschul SF, Madden TL, Schaffer AA, Zhang J, Zhang Z, Miller W, Lipman DJ. Gapped BLAST and PSI-BLAST: a new generation of protein database search programs. *Nucleic Acids Res*. 1997;25(17):3389-3402.
7. Zhang Y, Skolnick J. TM-align: A protein structure alignment algorithm based on TM-score. *Nucleic Acids Res*. 2005;33(7):2302-2309.
8. Terashi G, Takeda-Shitaka M. CAB-align: a flexible protein structure alignment method based on the

- residue-residue contact area. *PLoS One*. 2015;10(10):e0141440.
9. Kundrotas PJ, Anishchenko I, Dauzhenka T, Kotthoff I, Mnevets D, Copeland MM, Vakser IA. DOCKGROUND: a comprehensive data resource for modeling of protein complexes. *Protein Sci*. 2018;27(1):172-181.
 10. Roy Burman SS, Yovanno RA, Gray JJ. Flexible backbone assembly and refinement of symmetrical homomeric complexes. *Structure*. 2019;27(6):1041-1051.
 11. Dong GQ, Fan H, Schneidman-Duhovny D, Webb B., Sali A. Optimized atomic statistical potentials: assessment of protein interfaces and loops. *Bioinformatics*. 2013;29(24):3158-3166.
 12. Mukherjee S, Zhang Y. MM-align: a quick algorithm for aligning multiple-chain protein complex structures using iterative dynamic programming. *Nucleic Acids Res*. 2009;37(11):e83.

XIX. Modeling CAPRI and Oligomeric CASP Targets by Template-Based and Free Docking

Petras J. Kundrotas, Amar Singh, and Ilya A. Vakser

Computational Biology Program and Department of Molecular Biosciences, University of Kansas, Lawrence, KS, USA

We performed the initial alignment of the CAPRI and CASP targets by HHpred.¹ If the alignment had > 90% probability and covered > 80% of the target sequence, we utilized NEST² to build the protein models for the docking. Otherwise, we used CASP stage 2 server models of the individual proteins, except those with loose packing. For the template-based docking, the structure alignment by TM-align³ was scored by a combination of structure similarity metrics, normalized AACE18⁴ values for the interface, fraction of shared target/template contacts, target/template interface sequence identity, interface solvation score, and the extent of clashes in the unrefined predictions.⁵ The free docking by GRAMM was performed at lower resolution (3.5 Å grid step) to accommodate structural inaccuracies of the modeled proteins. The predicted matches were scored by the AACE18 potential. The text-mining procedure⁶ was used to identify the binding site residues, which served as additional docking constraints. All final predictions were minimized by TINKER.⁷ The results are summarized in Table 1.

Table 1. Docking of CASP14-CAPRI targets

CAPRI target	CASP target	Proteins	Organism	Assembly	Experimental method	Number of residues	Number of HHpred templates	Rank of the best model by CASP
T164	T1032	smchD1	Human	A2	X-ray	284	107	95
T165	H1036	Glycoprotein gB/antibody 93k	Varicella-zoster virus/human	A3B3C3	EM	622/128/106	9/250/250	N/A
T166	H1045	PEX4/PEX22	<i>Arabidopsis Thaliana</i>	A1B1	X-ray	157/173	22	19
T167	T1050	ATPase	<i>Bacteroides Ovatus</i>	A2	X-ray	779	250	N/A
T168	T1052	Tail spike protein	Salmonella phage epsilon15	A3	X-ray	832	250	11
T169	T1054	Outer-membrane lipoprotein	<i>Acinetobacter baumannii</i>	A2	X-ray	190	18	105
T170	H1060	tail subcomplex	T5 phage	A6B3C12D6	EM	464/298/140/204	11/1/4/6	9
T171	T1063	CCNB1IP1	Human	A4	X-ray	196	208	N/A
T172	H1066	CCPol/MP-2	-	A1B1	X-ray	366/123	11/0	
T173	H1069	CCPol/MP-1	-	A1B1	X-ray	369/122	11/0	
T174	T1070	Tail spike protein	Escherichia virus CBA120	A3	X-ray	335	2	11
T175	T1073	DUF4423	<i>Bdellovibrio bacteriovorus</i>	A4	X-ray	255	250	9

T176	T1078	Tsp1	<i>Trichoderma virens</i>	A2	X-ray	138	1	24
T177	H1081	Arginine decarboxylase	<i>Providencia stuartii</i>	A20	EM	758	250	N/A
T178	T1083	Nitro	<i>Nitrosococcus ocea</i>	A2	X-ray	98	0	48
T179	T1087	Tuna	<i>Methylobacter tundripaludum</i>	A2	X-ray	93	1	18
T180	T1099	Capsid protein	Duck hepatitis B virus	A?	EM	262	4	17
T181	H1103	Orf3a-HMOX1	SARS2-Human	A1B1	X-ray	275/288	1/37	N/A

Table 1. Continued

CAPRI target	CASP target	Proteins	Organism	Assembly	Experimental method	Number of residues	Number of HHpred templates	Rank of the best model by CASP
<i>CASP only oligomeric targets</i>								
	T1034	BIL2	<i>Tetrahymena thermophila</i>	A4	X-ray	156	0	41
	T1038	TSWV glycoprotein	Tomato spotted wilt virus	A2	X-ray	199	0	13
	H1047	FlgH-FlgI	<i>Shigella sonnei</i>	A1B1?	EM	232/365	1/0	7
	T1048	HD_1495	<i>Haemophilus ducreyi</i>	A4	X-ray	109	0	23
	T1061	tail subcomplex	T5 phage	A3	EM	949	192	36
	T1062	tail subcomplex	T5 phage	A3	EM	35	0	N/A
	H1065	Cytosine Methyltransferase	<i>Serratia marcescens</i>	A1B1	X-ray	127/98	0/0	8
	H1072	SYCE2/TEX12	Human	A2B2	X-ray	101/69	0/2	17
	T1080	Bd3182	<i>Bdellovibrio bacteriovorus</i>	A3	X-ray	922	129	14
	T1084	Meio	<i>Meiothermus silvanus</i>	A2	X-ray	73	0	48
	H1097	AR9	<i>Bacillus phage PBS1</i>	ABCDE	EM	426/631/49 6/665/464	14/16/0/12/0	44

For n -homomeric targets, we performed spatial rearrangement of the target protein to match the monomers in the experimentally determined complexes either from the full-structure template library⁸ or from an *ad hoc* library generated from PDB for a particular target. The *ad hoc* library contained structures which (a) were identified by the HHpred as likely templates (> 90% probability) and (b) had oligomeric state in the biounit corresponding to that of the target. For target T177/H1081, due to anticipated conformational changes and large size of the putative interface, the free docking of the two 10-mers was performed with C^α atoms only. For n -heteromeric targets, we looked for common HHpred templates, when the templates for the target monomers were identified either as interacting chains in a PDB entry, or non-overlapping parts of the same chain. If no reliable templates were found, we performed free docking, including cross-docking of all selected CASP stage 2 server models.

References

1. Remmert M, Biegert A, Hauser A, Soding J. HHblits: Lightning-fast iterative protein sequence searching by HMM-HMM alignment. *Nat Methods*. 2012;9:173-175.
2. Petrey D, Xiang ZX, Tang CL, et al. Using multiple structure alignments, fast model building, and energetic analysis in fold recognition and homology modeling. *Proteins*. 2003;53:430-435.
3. Zhang Y, Skolnick J. TM-align: A protein structure alignment algorithm based on the TM-score. *Nucl Acid Res*. 2005;33:2302-2309.
4. Anishchenko I, Kundrotas PJ, Vakser IA. Contact potential for structure prediction of proteins and protein

- complexes from Potts model. *Biophys J*. 2018;115:809-821.
5. Kundrotas PJ, Anishchenko I, Dauzhenka T, Vakser IA. Modeling CAPRI targets 110-120 by template-based and free docking using contact potential and combined scoring function. *Proteins*. 2018;86:302–310.
 6. Badal VD, Kundrotas PJ, Vakser IA. Text mining for protein docking. *PLoS Comp Biol*. 2015;11:e1004630.
 7. Ren P, Wu C, Ponder JW. Polarizable atomic multipole-based molecular mechanics for organic molecules. *J Chem Theory Comput*. 2011;7:3143-3161.
 8. Anishchenko I, Kundrotas PJ, Tuzikov AV, Vakser IA. Structural templates for comparative protein docking. *Proteins*. 2015;83:1563–1570.

XX. Modeling of protein complexes in CAPRI Round 50

Justas Dapkūnas, Kliment Olechnovič and Česlovas Venclovas

Institute of Biotechnology, Life Sciences Center, Vilnius University

Saulėtekio av. 7, LT-10257 Vilnius, Lithuania

ceslovas.venclovas@bti.vu.lt, justas.dapkunas@bti.vu.lt, kliment.olechnovic@bti.vu.lt

Methods

In CASP14-CAPRI round 50 we used the same general modeling workflow as in CASP13¹ with several improvements. For every target we initially attempted to identify multimeric templates. If sequence-based searches using PPI3D² and HHpred³ failed, we employed structure-based searches against PDB by submitting CASP server models to the DALI server⁴. If templates were identified, structural models were generated using MODELLER plugin AltMod^{5, 6}. Otherwise, free docking of five selected monomeric CASP server models was done using Hex⁷ for hetero-complexes and Sam⁸ for homomultimers. For some larger target protein complexes templates were available only for some of the subunits or domains. In such cases a hybrid strategy was used, where part of the complex was generated by homology modeling, whereas remaining subunits were docked either by simply using TM-align⁹ or by free docking. If the reliability of identified templates was questionable, we used a different hybrid strategy, performing both template-based modeling and free docking. In those cases we submitted best models generated by both approaches.

For model selection we utilized VoromQA¹⁰ taking into account both global scores and interface scores as described previously¹ with some modifications. More specifically, we used an improved version of VoromQA (VoromQA-dark) for global structure evaluation and an improved tournament-based ranking algorithm. Standard automated procedure was used to select the best template-based models and 10 best models in the CAPRI scoring challenge. In the case of free docking the top 100-500 selected models were subsequently relaxed by a very short molecular dynamics simulation using OpenMM¹¹ and then re-ranked. Constraints obtained from literature searches or CASP contact prediction servers, if available, were also used in selection of free-docking models. All models, resulting from both template-based modeling and free docking, were visually inspected before submission and, if necessary, their ranking was adjusted manually.

Results

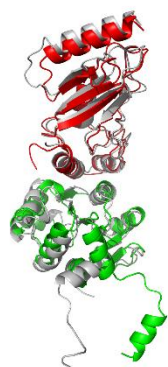
Our CAPRI results are summarized in Table 1 and two highlight cases are provided in Figure 1. We used template-based modeling for five, free docking for one and a hybrid approach for six targets. Template-based modeling usually resulted in models of acceptable or higher quality according to the CAPRI criteria¹² except for two cases. Of these two, the first one featured large insertions in the sequence-structure alignment corresponding to the interface region (interface No. 1 in T180, CASP T1099v1). The second case represents the failure to

identify the correct epitope in the antibody-antigen interaction (T165, CASP H1036v0). The success of free docking was mixed: sometimes models were completely incorrect (T169, CASP T1054), whereas sometimes docking outperformed the template-based approach (T178, CASP T1083; see Fig. 1). In the case of a large target (T170, CASP H1060), higher quality models were obtained for the interfaces that could be modeled using structural templates.

Table 1. Summary of the results obtained by the “Venclovas” group in modeling CAPRI targets

CASP Target	CAPRI Target	Template search methods	Notes	CAPRI evaluation of our best model	Maximum f_{nat}
Template-based modeling:					
T1032	T164	PPI3D, HHpred		acceptable	0.45
H1036v0	T165	PPI3D, HHpred	Antibody-antigen interface which is not conserved	incorrect	0
H1045	T166	HHpred		high	0.81
T1052	T168	PPI3D		medium	0.75
T1099	T180	PPI3D	Interface 1 had large insertions	incorrect/ medium	0.01-0.51
Hybrid modeling:					
H1060	T170	DALI		incorrect/ acceptable/ medium	0-0.61
T1070	T174	HHpred, PPI3D	Low resolution template and low quality alignment, reliable templates only for domains	incorrect	0.11
T1078	T176	DALI	A mixture of template-based and free docking models, the best model from docking	incorrect	0.36
H1081	T177	PPI3D	Free docking of two template-based 10mer models	medium/ high	0.50-0.84
T1083	T178	DALI	A mixture of template-based and free docking models, the best model from docking	medium	0.68
T1084	T179	DALI	A mixture of template-based and free docking models	acceptable	0.51
Free docking:					
T1054	T169			incorrect	0.02

CAPRI T166
CASP H1045



CAPRI T178
CASP T1083

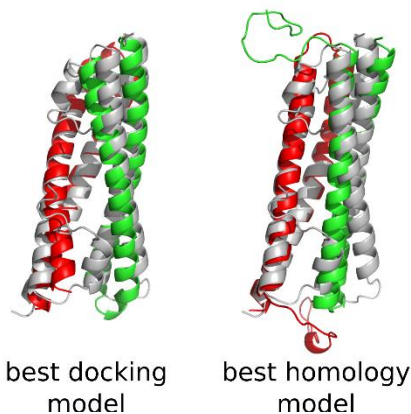


Figure 1. Top CAPRI results obtained by the “Venclovas” group: a template-based high quality model for T166 (CASP H1045) and the best models for T178 (CASP T1083). Model chains are colored green and red, and the experimental target structure is shown in grey.

Funding: Research Council of Lithuania (grant S-MIP-17-60).

References

1. Dapkūnas J, Olechnovič K, Venclovas Č. Structural modeling of protein complexes: Current capabilities and challenges. *Proteins* 2019;87(12):1222–1232.
2. Dapkūnas J, Timinskas A, Olechnovič K, Margelevičius M, Dičiūnas R, Venclovas Č. The PPI3D web server for searching, analyzing and modeling protein-protein interactions in the context of 3D structures. *Bioinformatics* 2017;33(6):935–937.
3. Zimmermann L, Stephens A, Nam S-Z, Rau D, Kübler J, Lozajic M, Gabler F, Söding J, Lupas AN, Alva V. A Completely Reimplemented MPI Bioinformatics Toolkit with a New HHpred Server at its Core. *J Mol Biol* 2018;430(15):2237–2243.
4. Holm L. DALI and the persistence of protein shape. *Protein Sci* 2020;29(1):128–140.
5. Šali A, Blundell TL. Comparative Protein Modelling by Satisfaction of Spatial Restraints. *J Mol Biol* 1993;234(3):779–815.
6. Janson G, Grottesi A, Pietrosanto M, Ausiello G, Guarguaglini G, Paiardini A. Revisiting the “satisfaction of spatial restraints” approach of MODELLER for protein homology modeling. *PLoS Comput Biol* 2019;15(12):e1007219.
7. Ritchie DW, Kemp GJ. Protein docking using spherical polar Fourier correlations. *Proteins* 2000;39(2):178–194.
8. Ritchie DW, Grudin S. Spherical polar Fourier assembly of protein complexes with arbitrary point group symmetry. *J Appl Cryst* 2016;49(1):158–167.
9. Zhang Y, Skolnick J. TM-align: a protein structure alignment algorithm based on the TM-score. *Nucleic Acids Res* 2005;33(7):2302–2309.
10. Olechnovič K, Venclovas Č. VoroMQA: Assessment of protein structure quality using interatomic contact areas. *Proteins* 2017;85(6):1131–1145.
11. Eastman P, Swails J, Chodera JD, McGibbon RT, Zhao Y, Beauchamp KA, Wang L-P, Simmonett AC, Harrigan MP, Stern CD, Wiewiora RP, Brooks BR, Pande VS. OpenMM 7: Rapid development of high performance algorithms for molecular dynamics. *PLoS Comput Biol* 2017;13(7):e1005659.
12. Méndez R, Lepplae R, De Maria L, Wodak SJ. Assessment of blind predictions of protein-protein interactions: current status of docking methods. *Proteins* 2003;52(1):51–67.

XXI. Summary of the Zou Group and the MDOCKPP server

Rui Duan¹, Liming Qiu¹, Xianjin Xu¹, Shuang Zhang¹, Jian Liu², Farhan Quadir², Raj Roy², Jianlin Cheng^{2,3}, Xiaoqin Zou^{1,3,4,5}

¹. Dalton Cardiovascular Research Center, University of Missouri, Columbia, Missouri, USA.

². Department of Electrical Engineering and Computer Science, University of Missouri, Columbia, Missouri, USA.

³. Institute for Data Science and Informatics, University of Missouri, Columbia, Missouri, USA.

⁴. Department of Physics and Astronomy, University of Missouri, Columbia, Missouri, USA.

⁵. Department of Biochemistry, University of Missouri, Columbia, Missouri, USA.

We participated in the joint CASP14-CAPRI experiment as both predictor and scorer in all the announced targets. Different from our approaches used in the previous CASP13-CAPRI experiment¹, in-house developed GPU version of MDockPP server^{2,3} and deep-learning-based DLScorePP scoring function were applied to the prediction of the binding modes in the current competition. In addition, a novel version of the MULTICOM-CLUSTER server⁴ was used to generate monomeric structures.

In the prediction challenge, templated-based and/or docking-based methods were applied depending on the features of the targets. Specifically, for a given target, the BLAST program⁵ was utilized to search for appropriate templates in the Protein Data Bank. If all the chains were found in a single PDB entry, the Modeller program⁶ was applied to build the structure of the target using the complex structure in this PDB entry as a template. On the other hand, if templates for different chains of a target were found in different PDB entries, the Modeller program was utilized to construct the monomeric structure of each chain. If no template was found, the structures of the monomers were generated using the CASP14 MULTICOM-CLUSTER server. Moreover, the 150 best monomeric structures for each target provided by CASP groups were also evaluated using both ITScorePro⁷ and DeepRank⁸⁻¹⁰. About 10 monomeric structures were selected using the consensus of these two scoring functions and biological information, which were then used as the input for docking with our MDockPP server.

Our in-house developed GPU version of the MDockPP server uses a fast Fourier transform (FFT)-based rigid docking algorithm¹¹ to generate putative binding modes. The biological information searched by an in-house Rebipp server³ were also used as an input for the MDockPP server. The generated binding poses were optimized and ranked with our ITScorePP scoring function¹², which is an atomic-level, statistical potential-based scoring function for protein-protein interactions. If a target is dimeric, the top ranked binding modes by ITScorePP were further ranked with our recently developed deep learning model called DLScorePP. Next, the ranked binding modes were clustered according to their RMSDs. The best model from each of the top 10-ranked clusters were selected and submitted to CAPRI as the MDOCKPP server prediction. For human prediction, up to 100 binding modes were manually inspected, and ten models were selected for CAPRI submission.

In the scoring experiment, the same protocol was used for both the server and human scoring challenge, except that now the putative binding modes were collected from the groups participating in the docking experiment and redistributed by CAPRI.

In CASP14-CAPRI, our human prediction ranked at the #4 position in the prediction category and MDockPP ranked at the #1 position in the server prediction category, according to the preliminary assessment released by CAPRI in December 2020. Specifically, our human group (server) produced models of at least acceptable quality for 8 (7) out of 14 targets/interfaces whose structures are solved. Our server achieved high-accuracy prediction for T177. The performance of the MDockPP server is approaching to the performance of our human prediction. In the scoring category, our human and server (MDOCKPP) scoring prediction both ranked at the first positions when the Top-5 models are considered; our human (server) groups produced models of at least acceptable quality for 10 (9) out of 14 targets/interfaces with solved structures (including the three sub-targets of T170). The performance of our group for each target is summarized in Table 1. Similar with the previous CASP13-CAPRI experiment, the major difficulties are 1) how to further improve the acceptable accuracy models to medium or high accuracy models, and 2) how to make the rigid docking algorithm less sensitive to the conformations of monomeric structures.

Funding information: Xiaoqin Zou is supported by NIH grants R01GM109980 (PI: Xiaoqin Zou), NIH R35GM136409 (PI: Xiaoqin Zou) and NIH R01HL142301 (PI: Johnathan R. Silva).

Reference

1. Lensink MF, Brysbaert G, Nadzirin N, et al. Blind prediction of homo- and hetero-protein complexes: The CASP13-CAPRI experiment. *Proteins Struct Funct Bioinforma*. 2019;87(12):1200-1221. doi:10.1002/prot.25838
2. Xu X, Qiu L, Yan C, Ma Z, Grinter SZ, Zou X. Performance of MDockPP in CAPRI rounds 28-29 and

- 31-35 including the prediction of water-mediated interactions. *Proteins Struct Funct Bioinforma.* 2017;85(3):424-434. doi:10.1002/prot.25203
3. Duan R, Qiu L, Xu X, et al. Performance of human and server prediction in CAPRI rounds 38- 45. *Proteins Struct Funct Bioinforma.* 2020;88(8):1110-1120. doi:10.1002/prot.25956
 4. Liu J., Wu T., Guo Z., Hou J., Cheng J. Improving protein tertiary structure prediction by deep learning and distance prediction in CASP14. *bioRxiv.* 2021. doi: <https://doi.org/10.1101/2021.01.28.428706>
 5. Altschul SF, Madden TL, Schäffer AA, et al. Gapped BLAST and PSI-BLAST: A new generation of protein database search programs. *Nucleic Acids Res.* 1997;25(17):3389-3402. doi:10.1093/nar/25.17.3389
 6. Martí-Renom MA, Stuart AC, Fiser A, Sánchez R, Melo F, Šali A. Comparative Protein Structure Modeling of Genes and Genomes. *Annu Rev Biophys Biomol Struct.* 2000;29(1):291-325. doi:10.1146/annurev.biophys.29.1.291
 7. Huang SY, Zou X. ITScorePro: An efficient scoring program for evaluating the energy scores of protein structures for structure prediction. *Methods Mol Biol.* 2014;1137:71-81. doi:10.1007/978-1-4939-0366-5_6
 8. Hou J, Wu T, Cao R, Cheng J. Protein tertiary structure modeling driven by deep learning and contact distance prediction in CASP13. *Proteins Struct Funct Bioinforma.* 2019;87(12):1165-1178. doi:10.1002/prot.25697
 9. Cao R, Bhattacharya D, Adhikari B, Li J, Cheng J. Massive integration of diverse protein quality assessment methods to improve template based modeling in CASP11. *Proteins Struct Funct Bioinforma.* 2016;84(S1):247-259. doi:10.1002/prot.24924
 10. Cao R, Bhattacharya D, Adhikari B, Li J, Cheng J. Large-scale model quality assessment for improving protein tertiary structure prediction. In: *Bioinformatics.* Vol 31. Oxford University Press; 2015:i116-i123. doi:10.1093/bioinformatics/btv235
 11. Chen R, Li L, Weng Z. ZDOCK: An initial-stage protein-docking algorithm. *Proteins Struct Funct Genet.* 2003;52(1):80-87. doi:10.1002/prot.10389
 12. Huang S-Y, Zou X. An iterative knowledge-based scoring function for protein-protein recognition. *Proteins Struct Funct Bioinforma.* 2008;72(2):557-579. doi:10.1002/prot.21949

Table 1. List of templates and target performance of our group.

Target	Possible templates*	Stoichiometry	Best prediction of our Top-5 models			
			Prediction		Scoring	
			Server	Human	Server	Human
T164	1gxl	A2	Medium	Acceptable	Medium	Acceptable
T165	5ys6, 5avg	A:HL	Incorrect	Incorrect	Incorrect	Incorrect
T166	2oxq	AB	Acceptable	Medium	Medium	Medium
T167	-	Cancelled	-	-	-	-
T168	6f7k	A3	Medium	Medium	Medium	Medium
T169	1fg9	A2	Incorrect	Incorrect	Incorrect	Incorrect
T170.1		A6B12C3D6	Medium	Medium	Acceptable	Medium
T170.2			Incorrect	Incorrect	Incorrect	Incorrect
T170.3			Acceptable	Acceptable	Acceptable	Acceptable
T170.4			Incorrect	Incorrect	Incorrect	Acceptable
T170.5			Incorrect	Incorrect	Medium	Medium
T170.6			Incorrect	Incorrect	Incorrect	Incorrect
T170.7			Incorrect	Incorrect	Incorrect	Incorrect
T170.8			Incorrect	Incorrect	Acceptable	Acceptable
T170.9			Incorrect	Incorrect	Acceptable	Acceptable
T171	-	No structure	-	-	-	-
T172	-	No structure	-	-	-	-
T173	-	No structure	-	-	-	-
T174		A3	Incorrect	Incorrect	Incorrect	Incorrect
T175	-	Cancelled	-	-	-	-
T176		A2	Acceptable	Acceptable	Acceptable	Acceptable
T177.1		A10:A10	High	High	High	High
T177.2			High	High	High	High
T177.3			High	Medium	Medium	Medium
T178		A2	Acceptable	Acceptable	Acceptable	Acceptable
T179		A2	Acceptable	Acceptable	Acceptable	Acceptable
T180.1		A2:A2	Incorrect	Incorrect	Incorrect	Incorrect
T180.2			Acceptable	Medium	Medium	Medium
T181	3czy, 1ni6	No structure	-	-	-	-

*Only the templates used for homology modeling with the Modeller program are listed.